Title
Septin Function in T Lymphocyte Crawling and Structural Integrity

Permalink
https://escholarship.org/uc/item/4sh9p6tk

Author
Tooley, Aaron J

Publication Date
2007-05-08

Peer reviewed|Thesis/dissertation

Septin Function in T Lymphocyte Crawling and Structural Integrity

by

Aaron J. Tooley

DISSERTATION

Submitted in partial satisfaction of the requirements for the degree of

DOCTOR OF PHILOSOPHY

in

Biomedical Sciences

in the

GRADUATE DIVISION

of the

UNIVERSITY OF CALIFORNIA, SAN FRANCISCO

Acknowledgements

In my time in graduate school, I have met many people who have helped me with both personal and scientific advice. Without the help of these people, I would probably not be writing these acknowledgements today. First, I would like to thank my advisor Max Krummel for supporting my graduate work. In the past five years, I have learned a lot from Max, including how to be a successful scientist. Max has also done his best to make sure the lab was both a good and fun place to work. I would also like to thank members of my thesis committee, Art Weiss and Mike McManus, who have guided my passage through graduate school.

In my five years in the Krummel lab, I have had the opportunity to work with many great people and would like to thank both current and former members of the lab. In particular, I would like to thank Jordan Jacobelli, Priya Pandurangi, and Chris Bennett. Jordan has been instrumental in my graduate career and has always acted like a second mentor to me. Priya and Chris were always there to listen and provide helpful advice. In addition, I would also like to thank Sumone Chakravarti, a former bench mate who made lab life a little more enjoyable. Finally, I would like to thank my friend and classmate Chris Allen, who has provided both guidance and support throughout my entire graduate career.

Most research is not performed in a bubble and that is especially true for my graduate work. I would like to thank our collaborators Makato Kinoshita and Bill Trimble – without their help and reagents, the experiments presented in this thesis could not have been performed. I would also like to thank Shuwei Jiang and Cliff McArthur for technical

The studies presented in this thesis were performed under the guidance of Dr. Matthew F. Krummel. Chapter 3 of this thesis is based on a manuscript that will be submitted for publication, entitled "Annular and cortical septins act as structural scaffolds to maintain shape and limit protrusions in T lymphocytes." The following co-authors contributed to this work: Jordan Jacobelli, William S. Trimble (University of Toronto, Toronto, Canada), Makoto Kinoshita (Kyoto University, Kyoto, Japan) and Matthew F. Krummel.

Septin Function in T Lymphocyte Crawling and Structural Integrity

by

Aaron J. Tooley

Abstract

T lymphocytes are components of the adaptive immune response that circulate throughout the body in search of antigen presenting cells bearing peptide-MHC complex molecules. T cells are inherently polarized with an anterior leading edge and a posterior protrusion called the uropod. While several details of T cell polarity have been established, the source and significance of this morphology is still not completely understood. Septins are components of the cytoskeleton important for structural integrity and cell cycle control. They form heteromeric complexes that interact with both actin filaments and microtubules and have diverse biological functions. Therefore, we decided to investigate the role of septins in T cell morphology.

Septin complexes are found at the cell cortex and are enriched at the T cell mid-body. In order to assess the functional requirements of septins in T cells, we designed short hairpin RNAs (shRNAs) targeting Septins 1, 6, 7 and 9. Targeting of Sept7 resulted in the reduction of the entire septin complex, a result that was only observed when Sept7 was targeted. T cells lacking septin complexes have a pronounced increase in uropod length. To determine a potential mechanism for this result, we examined the activation state of myosin II in septin deficient T cells. In these cells, we did not observe any differences in

the phosphorylation of either the myosin light chain or heavy chain, although myosin II activity was still required for uropod formation.

Although septin deficient T cells crawled at normal velocities, they exhibited structural instabilities including membrane blebbing and the presence of excess protrusions. Septin deficient T cells also had a slight reduction in actin filaments. Therefore, it is not clear if the membrane defects we observed during crawling are from the reduction in actin filaments, reduction in the septin cytoskeleton or a combination of both. Finally, loss of septins did not affect functions that require cell polarization; however, septin deficient T cells rapidly permeated extremely small pores, consistent with the loss of a structural scaffold. Thus, septins play a critical role in T cell morphology and structural integrity and may be important for transendothelial migration.

Table of Contents

List of Figures

List of Tables

Chapter 3

Chapter 1:

T Lymphocyte Crawling and Morphology

Introduction

The immune system is the body's defense against foreign invaders such as pathogenic
bacteria, viruses, parasites and fungi. Although humans can live without an immune
system, they are extremely susceptible to infections and, depending on the severity of the
immunodeficiency, may require bone marrow transplants in order to survive. An
infection in a healthy person can be life threatening in patients with an immunodeficiency.
Mice that lack immune systems are also viable, but must be housed in pathogen-free
facilities in order to survive and often require antibiotics to stay healthy. The immune
system is made up of white bloods cells (or leukocytes) that circulate through the blood,
secondary lymphoid organs (spleen and lymph nodes), and sites of antigen entry (skin,
mucous membranes and the gastrointestinal tract). T lymphocytes or T cells are part of
the adaptive immune response and play a key role in the recognition and elimination of
pathogens.

T cell progenitors leave the bone marrow and travel via the bloodstream to the thymus
where they mature (hence the name "thymus" or "T" cells). T cells express receptors
specific for peptides presented on major histocompatibility complex (MHC) molecules. T
cell development in the thymus involves both positive and negative selection in order to
produce T cells that can recognize foreign antigens presented on MHC molecules.
Through differential rearrangements of gene segments, the immune system can generate
T cells specific for millions of different foreign peptide-MHC molecules. Negative
selection of thymocytes also prevents the production of T cells that recognize self-
peptides too strongly, which can lead to autoimmune diseases.

2

T cells that are positively selected leave the thymus and enter the bloodstream. Once in the bloodstream, they circulate and enter secondary lymphoid organs in search of antigens, which are trafficked to these organs by dendritic cells for presentation to T cells. This allows T cells to efficiently scan for antigens in specific locations instead of having to search the entire body for pathogens. If a T cell encounters its cognate antigen on an antigen-presenting cell, it becomes activated through a series of signaling pathways that ultimately leads to proliferation, differentiation and gain of effector functions. The activated T cell then exits the lymph node, re-enters the bloodstream and traffics to sites of inflammation. If a T cell does not encounter its cognate antigen, it eventually exits the lymph node, re-enters the bloodstream, but traffics to other secondary lymphoid organs in search of foreign peptides.

T cell polarity

T cells circulating in the blood have a rounded-spherical morphology; however, when T cells exit the blood and enter tissues, chemotactic signals induce dramatic changes in the T cell cytoskeleton resulting in a highly polarized morphology. This polarity is required for the high motility and directional crawling observed for T cells both *in vitro* and *in vivo*. Polarized T cells exhibit a classic 'hand-mirror' morphology that is characterized by an anterior leading edge at the front of the cell body and a posterior protrusion called the uropod. The leading edge is characterized by the formation of lamellipodia and filopodia and is the predominant site of actin protrusions in polarized T cells (Sanchez-Madrid and del Pozo, 1999). In addition, chemokine receptors have been shown to localize to the

3

leading edge. At the back of the polarized T cell, the uropod is characterized by the presence of adhesion molecules, including CD43, CD44 and ICAMs. These molecules are connected to the actin cytoskeleton through linker proteins of the ezrin/radixin/moesin (ERM) family of proteins, which also localize to the uropod.

The nucleus in polarized T cells is found directly behind the leading edge and occupies most of the cell body, while the majority of the cytoplasm is found in the uropod. In polarized (and crawling) T cells, the microtubule-organizing center (MTOC) is located behind the nucleus in the cytoplasm rich uropod. This is in contrast to what is observed for fibroblasts (Cau and Hall, 2005; Gomes et al., 2005), which polarize their MTOC in front of the nucleus for directional migration. The microtubule network has also been proposed to play a role in T cell polarity, possibly through the targeting of vesicles to the leading edge during crawling (reviewed in Krummel and Macara, 2006).

T cell polarity requires both signaling pathways and an intact actin cytoskeleton (Lee et. al., 2004), since the uropod is lost in cells treated with either staurosporine (a general kinase inhibitor) or cytochalasin D (an actin depolymerizing agent). T cell polarity is regulated by the Rho family of GTPases (reviewed in Raftopoulou et al., 2004), including Rho, Rac and Cdc42. Actin polymerization at the leading edge is regulated by Rac (for lamellipodia) and Cdc42 (for filopodia), while actin-myosin (actomyosin) contraction in the T cell mid-body and uropod is regulated by Rho. Consequently, Rho activation is required for uropod formation. The role of these molecules in T cell crawling is discussed in the next section.

In the polarized T cell lymphoma cell line EL4, formation of the uropod required activation of Rho and its downstream effector ROCK (Lee et al., 2004). Over-expression of a dominant-negative Rho or treatment of T cells with the ROCK inhibitor Y-27632 resulted in loss of the uropod. This correlates well with the physical location of Rho activation, as expression of a constitutively active Rho was found to accumulate in the uropod. Interestingly, inhibition of the Rho/ROCK signaling pathway did not disrupt membrane polarity, as a polarized 'uropodal cap' (containing CD44 and phosphorylated ERM proteins) was still present in Y-27632 treated cells. This indicates that although the Rho/ROCK pathway is required for uropod formation in T cells, it is not required to establish membrane polarity.

In the EL4 system, polarized cap formation correlated with phosphorylation of ERM proteins (Lee et al., 2004). Treatment of wild-type cells with staurosporine resulted in loss of both the uropod and the polarized cap. However, cells expressing an ezrin mutant (T567D) that mimics phosphorylation (active form) maintained the polarized cap after addition of staurosporine, supporting a role for ezrin in establishing membrane polarity. In addition, the T567D mutant was predominantly found in the uropod and over-expression of this mutant resulted in increased uropod length, which correlated with an increase in active Rho (Rho-GTP). Therefore, uropod formation requires both phosphorylation of ERM proteins, to establish membrane polarity, and activation of Rho and its downstream effector ROCK, to generate the contractile force need to generate the uropod.

In epithelial cells, a network of polarity proteins including Scribble, Crumbs3 and Par3 (all of which are part of multi-protein complexes) are important for apical-basolateral polarity. Recently, these molecules were shown to be required for T cell polarity (Ludford-Menting et al., 2005) and these proteins most likely function to define specific regions of the T cell membrane. In flies, Scribble has been genetically linked to two other polarity proteins: Dlg and Lgl. In crawling T cells, Scribble and Dlg1 are localized in the uropod. shRNA knock-down of Scribble resulted in T cell rounding and loss of the uropod. Similar results were obtained when a blocking fragment of Dlg was over-expressed in T cells. In cells lacking Scribble, both ezrin and CD44 were evenly distributed around the cell, indicating not only the loss of the uropod, but loss of membrane polarity as well.

From this data, the following model for formation of the uropod can be proposed. Scribble and Dlg define a distinct region of the membrane and are required to establish membrane polarity, a process that requires the actin cytoskeleton. Once membrane polarity is established, ERM proteins are phosphorylated in the uropod resulting in localized activation of Rho and its downstream effector ROCK. Activation of ROCK results in activation of myosin II, which leads to contraction of actomyosin filaments and, hence, uropod formation. This model correlates well with the physical location of myosin II (Jacobelli et al., 2004; Ratner et al., 2003), which has been shown to accumulate in the T cell mid-body/uropod. Consequently, treatment of T cells with the myosin II inhibitor Blebbistatin resulted in T cell rounding and loss of the uropod (Jacobelli et al., 2004).

T cell crawling

A T cell migrates via a coordinated series of events that require dynamic changes in the actomyosin cytoskeleton (reviewed in Raftopoulou et al., 2004). The driving force for migration involves actin protrusions at the leading edge or lamellipodia followed by contraction at the cell mid-body. Once new adhesion sites are established at the front of the cell, contraction pushes the contents of the cell forward and subsequent release of adhesions at the rear results in forward motion. In T cells, this process is coordinated such that T cell morphology is maintained during crawling. This form of migration is also known as amoeboid migration (based on similarities to the amoeba *Dictyostelium discoideum*) and does not involve degradation of the extracellular matrix (ECM) (reviewed in Friedl, 2004). The high motility observed for T cells is achieved through short-weak interactions with the substratum, as opposed to other cell types that adhere more strongly to the ECM.

T cell crawling is controlled by many of the same players involved in determining T cell polarity. This is especially true for Rho, Rac and Cdc42, which coordinate actin protrusions at the leading edge (Rac and Cdc42) with actomyosin contraction in the T cell mid-body/uropod (Rho). Rac and Cdc42 activate downstream signaling cascades that result in actin polymerization at the leading edge (reviewed in Raftopoulou et al., 2004; Schwartz, 2004). Both Rac and Cdc42 have been shown to activate p21-associated kinases (PAKs), which regulate actin polymerization through LIM kinase and its downstream target cofilin. Cofilin cycles between active and inactive states depending on

phosphorylation, and this dynamic is important for both stabilizing pre-existing actin filaments and generating new ones (reviewed in Samstag et al., 2003). In the inactive form (phosphorylated), cofilin stabilizes actin filaments, while in the active form (non-phosphorylated), cofilin severs pre-existing actin filaments to generate more free ends for actin polymerization.

Rac and Cdc42 also interact with members of the WASP/SCAR/WAVE family of proteins, which act as scaffolds for actin polymerization (reviewed in Krummel and Macara, 2006; Raftopoulou et al., 2004). Cdc42 directly binds WASP, which activates the Arp2/3 complex responsible for both de novo actin polymerization and extension of already existing filaments. WASP activation also requires PIP_2 as a cofactor. Rac indirectly activates WAVE through interactions with an adaptor protein Nck, again resulting in activation of the Arp2/3 complex and actin polymerization.

While Rac and Cdc42 promote actin polymerization at the leading edge, Rho and its downstream effector ROCK, regulate contraction of actomyosin filaments in the T cell mid-body/uropod (reviewed in Raftopoulou et al., 2004). This process involves activation of myosin II through phosphorylation and deactivation of the myosin light chain (MLC) phosphatase. Increased phosphorylation of the MLC results in enhanced myosin motor activity, which leads to bundling and contraction of actin filaments. Tightening of actomyosin filaments provides tension and promotes forward movement of the cell body. Consequently, myosin II activity is required for T cell crawling (Jacobelli et al., 2004).

T cell crawling *in vivo*

While T cell crawling has mainly been studied *in vitro*, advances in two-photon microscopy have allowed researchers to study T cell motility *in vivo* in intact lymph nodes. In a seminal paper by Miller et al., three-dimensional T cell motility was observed in real-time, deep within whole explanted lymph nodes (Miller et al., 2002). Naïve T cells were purified from donor mice, labeled with fluorescent dyes and adoptively transferred into recipient mice for imaging. *In vivo*, T cells exhibited the same polarized hand-mirror morphology as observed for T cells *in vitro*. T cells on average crawled at ~11 µm/min with peak velocities greater than 25 µm/min. Although slightly higher, this velocity correlates well with what is observed for T cell crawling *in vitro*. In addition, T cell crawling was dynamic, characterized by a series of go, stop, go motions in which polarized T cells crawled for a given period of time before stopping and rounding up. This dynamic movement is also observed for T cell crawling *in vitro*.

In vivo, T cells are primarily found in the paracortex or T cell zone of lymph nodes (reviewed in Ebert et al., 2005). Segregation of the lymph node is achieved through localized production of chemokines and differential expression of chemokine receptors on distinct cell types. T cell homing to the T cell zone in lymph nodes requires expression of the chemokine receptor CCR7, whose ligands SLC and ELC are mainly expressed in the T cell zone. Although chemokine gradients are required for T cell homing to the paracortex, T cell crawling *in vivo* was characterized as a random walk (Miller et al., 2002), suggesting that chemokine gradients do not control T cell migration in the T cell zone. However, a recent study has implicated the role of fibroblastic reticular cells in

confining T cell movement within the paracortex (Bajenoff et al., 2006), questioning whether T cell migration *in vivo* is indeed random.

Transendothelial migration

In order for T cells to exit the blood and enter lymph nodes, they must pass through endothelial cells that line blood vessels, a process also known as transendothelial migration (reviewed in Ebert et al., 2005). This three-step process involves interactions between T cells and the endothelial cells. Entry into lymph nodes only occurs at specific locations along blood vessels, also known as high-endothelial venules (HEVs). The initial contact between a T cell traveling in the blood and HEVs results in T cell rolling along the endothelial cells. This process requires expression of adhesion molecules on both the surface of the T cell (L-selectin and β1-integrins) and on the surface of the endothelial cells (peripheral node-addressins or PNAds).

T cell rolling is followed by firm adhesion to the endothelium, a process that requires chemokine receptor signaling and results in increased affinity/avidity of integrins on the surface of the T cell. If chemokine levels are not sufficient, fluid force will cause the T cell to roll past the HEVs and re-enter the bloodstream. HEVs display and express chemokines (SLC and ELC) required for transendothelial migration by T cells. With chemokine signals, T cells flatten and cross the endothelial layer, a process also known as extravasation or diapedesis (reviewed in Ebert et al., 2005). Extravasation is mediated by integrins and adhesion molecules usually found at the junction between endothelial cells (reviewed in Nourshargh and Marelli-Berg, 2005). These junction proteins, which

include PECAM-1, CD99 and members of the JAM family, are also expressed on T cells and are required for extravasation. T cells mainly migrate through the junction between endothelial cells (paracellular migration); however, some leukocytes have been shown to actually migrate through the endothelial cell body (Hordijk, 2006), a process known as transcellular migration. Although the actin cytoskeleton is required for extravasation, dynamic changes that occur in the T cell cytoskeleton during this process are not well understood.

Conclusion

T cell polarity and crawling is determined by a complex interplay of signaling molecules that include members of the Rho family of GTPases, structural proteins and proteins involved in polarity determination. This polarity is required for efficient migration both *in vitro* and *in vivo*, the latter of which is essential for T cells to efficiently patrol the body in search of foreign pathogens. Although many aspects of T cell polarity have been determined, many mechanistic details remain unresolved. Septins are a family of proteins originally identified in budding yeast (reviewed in Kinoshita et al., 2006), and are involved in polarized growth of the bud during cell division. Several septins are highly expressed in lymphoid tissues (Hall et al., 2005); however, the role of septins in T cell polarity and crawling has not been investigated.

Chapter 2:

Septins: Components of the Cytoskeleton with Diverse Functions

Introduction

Septins are a class of GTP binding proteins that were first discovered in the budding yeast, *Saccharomyces cerevisiae* (Koshland et al., 1985). While conducting classical genetic screens in *S. cerevisiae*, Lee Hartwell identified over one hundred genes involved in control of the cell cycle. Mutant alleles of four of these cell division cycle genes (*cdc*), *cdc3, 10, 11* and *12*, were identified as temperature-sensitive mutants that caused defects in cytokinesis and septation (reviewed in Versele and Thorner, 2005). For this reason, they were later termed septins. Although *S. cerevisiae* encode seven septins, these four were the first to be identified. In addition to yeast, septins are found in most eukaryotes, but are absent in higher plants (Kinoshita, 2006). The number of septin genes varies in different organisms: five septins have been identified in Drosophila, two in *C. elegans*, at least 13 in humans and at least 12 in mice.

Septins are components of the cytoskeleton and are important for cell cycle control and vesicle trafficking, and act as diffusion barriers and plasma membrane scaffolds. They interact with both actin filaments and microtubules and function in remodeling of the cytoskeleton. Septins hetero-oligomerize to form higher order structures both *in vitro* and *in vivo*. They contain a classic GTP-binding domain and, although they possess GTPase activity, this is not thought to be a major component of their function as they do not rapidly hydrolyze GTP (reviewed in Hall and Russell, 2004). This result has led to the hypothesis that nucleotide binding is a structural element important for the formation of septin complexes. Septins are an interesting family of molecules whose diverse functions are not fully understood.

Structure of septin monomers

The primary structure of septin monomers is highly conserved throughout evolution

(reviewed in Versele and Thorner, 2005). Therefore, in this discussion, focus will be

placed on the structure of mammalian septins (human and mouse). The primary structure

of a septin monomer is shown in Figure 1a. All septins contain a core domain that

consists of a GTP-binding domain (from the P-loop superfamily), a septin-unique

element and a polybasic region that binds membrane phospholipids called

phosphatidylinositol (PtdIns) phosphates. In humans, the polybasic region binds

PtdIns(4,5)-bisphosphate (PIP$_2$) and PtdIns(3,4,5)-triphosphate (PIP$_3$), while in yeast this

region binds PtdIns(4)P and PtdIns(5)P (reviewed in Spiliotis and Nelson, 2006). Finally,

septins contain variable N-terminal and C-terminal extensions and have been grouped

phylogenetically based on the homology of their C-terminal tails.

Mammalian septins have been classified into three distinct groups based on homology of

the C-terminal variable regions (reviewed in Hall et al., 2005; Russell and Hall, 2005;

Spiliotis and Nelson, 2006; Versele and Thorner, 2005). The majority of septin

monomers contain a coiled-coil domain in their C-terminal tail and are grouped based on

the length of this domain. Members of the Septin 2 (Sept2) group (Septins 1, 2, 4, 5, 7

and 13) have shorter coiled-coil regions than members of the Sept6 group (Septins 6, 8,

10 and 11). Members of the Sept3 group (Septins 3, 9 and 12) do not contain coiled-coil

domains in their C-terminus. It should be noted that, although Sept7 and Sept13 are

closely related to Sept2 (Hall et al., 2005) and are now included in the Sept2 group, they

14

may be distinct from other members of this group as, until recently, they were classified as a fourth group by themselves. Finally, Septins 4, 8 and 9 contain a proline-rich domain in their N-terminal variable regions.

Septins form higher order complexes both *in vitro* and *in vivo*

The presence of higher order septin complexes has been verified in several different systems (Kinoshita et al., 2002; Kremer et al., 2005; Nagata et al., 2004; Sheffield et al., 2003; Surka et al., 2002). Immunoprecipitation of either Sept2 or Sept6 in HeLa cells resulted in the isolation of a septin complex that included Septins 2, 6 and 7 (Kinoshita et al., 2002; Kremer et al., 2005). When these septins were over-expressed in insect cells a complex with a 2:2:2 stoichiometric ratio was observed (Kinoshita et al., 2002). In fibroblasts, immunoprecipitation of Sept7 resulted in the purification of a larger septin complex that included at least Septins 2, 7, 8, 9 and 11 (Nagata et al., 2004). From these various systems, it has been hypothesized that Sept7 is central to the septin complex and may act as a core to which other septins are added (Figure 1b) (Kremer et al., 2005; Nagata et al., 2004).

In vitro pull-down assays have been used to map the interacting domains of septin monomers in higher order septin complexes. Nagata et al. used GST and MBP fusion proteins to map the interacting domains of Septins 7, 9 and 11 (Nagata et al., 2004). They showed that Sept7 interacts with both Sept9 and Sept11 through its C-terminal coiled-coil domain and that Sept11 showed the same pattern of binding to Sept7 and Sept9. In addition, they showed that Sept9 interacts with both Sept7 and Sept11 through its N-

terminal proline-rich domain; Sept9 is a member of the Sept3 group, which lack C-terminal coiled-coil domains.

Interestingly, the stability of the septin monomers appears to be dependent on the stability of the septin complex (Kinoshita et al., 2002; Kremer et al., 2005; Spiliotis et al., 2005). In fibroblasts, siRNA knock-down of Sept2 resulted in the reduction of Sept7 as well (Kinoshita et al., 2002). In this system, this result was not unique to Sept2, as a reciprocal depletion was observed when Sept7 was targeted (Sept2 was reduced). Similar results were seen in HeLa cells (Kremer et al., 2005), where siRNA targeting of Sept7 resulted in the reduction of Sept2 and Sept6. The reciprocal depletion was also seen as knock-down of Sept6 resulted in the reduction of Sept2 and Sept7. Co-regulation has also been observed in Sept5 knock-out (KO) mice (reviewed in Hall and Russell, 2004). In these animals, expression of Sept2 was up-regulated while expression of Sept7 was down-regulated. Although sufficient detail is known about the composition of septin complexes and how individual monomers interact to form these larger structures, the functional role of septin complexes *in vivo* has mainly been studied in budding yeast. The importance of these structures in other systems is not well established.

Septins are required for cell division in *S. cerevisiae*

In budding yeast, septins form filaments that can be arranged in linear arrays, coils, rings and gauzes (flat, interwoven arrays) (Rodal et al., 2005) and are important for multiple aspects of cell division. During the cell cycle, septins form a patch/ring at the presumptive bud site in late G1 (reviewed in Kinoshita, 2006). As the cell cycle

progresses into S phase and the bud emerges, the septins form a collar at the mother-bud neck. Once assembled, they direct polarized growth into the bud. At the start of mitosis (end of G2), the collar elongates into an hourglass structure and finally, the septin rings split during cytokinesis. At each of these points in the cell cycle, septins act as plasma membrane scaffolds to recruit molecules to the bud neck (reviewed in Kinoshita, 2006; Versele and Thorner, 2005) and act as diffusion barriers to confine these molecules to the area around the cleavage furrow (Dobbelaere and Barral, 2004).

Septins act as a scaffold to attract signaling proteins required for cell division to the mother-bud neck (reviewed in Kinoshita, 2006; Versele and Thorner, 2005). In budding yeast, septin rings are required to localize at least 21 proteins to the mother-bud neck and disruption of septin collar assembly delays the cell cycle at G2 (morphogenesis checkpoint). During G2, septins also act as a scaffold for components of the actomyosin ring complex, which are required for contraction during cytokinesis. When the septin rings split the actomyosin ring contracts to pinch off the daughter cell. Finally, septins are also required for abscission (the physical separation of two cells) in budding yeast. The exocyst complex, important for vesicle delivery and fusion, is also required for abscission and is recruited to the mother-bud neck. These data have led to the hypothesis that septins act as a scaffold to recruit the exocyst complex to the mother-bud neck and that vesicle fusion is required to provide new membrane during plasma membrane contraction and resolution (Dobbelaere and Barral, 2004).

In an elegant series of experiments using fluorescence recovery after photobleaching (FRAP) and a temperature-sensitive septin mutant Cdc12-6, Dobbelaere et al. demonstrated that during cytokinesis, septins not only act as a scaffold to recruit proteins to the cleavage furrow, they also act as a diffusion barrier to confine them there (Dobbelaere and Barral, 2004). Proteins freely diffused within the region confined by the septin rings, but not out of this compartment. Interestingly, while some proteins were confined to this region, others were free to shuttle in and out of the bud-neck. It is not clear how (or why) some proteins can pass the septin diffusion barrier while others cannot. In addition to confining proteins to the bud-neck, septins have also been shown to be important for creating a diffusion barrier between mother and daughter cell plasma membranes.

Budding yeast segregate RNA in order to create asymmetric protein distributions (Takizawa et al., 2000). This is accomplished by transporting the RNA molecules to distinct regions, for example the bud tip, in order to confine translation to a given region. This process requires actin filaments, motor proteins and adapter molecules that bind the RNA. In *S. cerevisiae*, the transmembrane protein IST2 (increased sodium tolerance) is one such protein whose RNA is transported to the bud tip, thus confining the protein to the daughter cell membrane during cell division. Using GFP-tagged IST2 and the temperature-sensitive septin mutant Cdc12-6, Takizawa et al. demonstrated that septins act as a diffusion barrier to confine IST2 to the daughter cell (Takizawa et al., 2000). When *cdc12-6* cells expressing Ist2-GFP were moved to a restrictive temperature, the diffusion barrier was lost and Ist2-GFP was no longer confined to the daughter cell

membrane. Loss of the septin diffusion barrier did not affect transport of IST2 RNA to the bud tip. Interestingly, during cell division, septins separate dividing yeast into three distinct compartments, the mother cell's plasma membrane, the junction at the mother-bud neck and the daughter cell's plasma membrane.

The dynamics of septin complexes vary throughout the cell cycle. In late G1 when the septins form a patch at the presumptive bud site and during cytokinesis when the septin rings split, FRAP studies have shown that septin structures are dynamic and freely exchange with septin monomers in the cytoplasm (Dobbelaere and Barral, 2004). However, during S phase, G2 and at the start of mitosis, septins rings are stable and do not exchange monomers in FRAP studies. In yeast, septin assembly and disassembly is controlled by phosphorylation and de-phosphorylation of septin subunits (reviewed in Kinoshita, 2006).

A complex network of signaling pathways regulates the formation, positioning and stability of septin rings (reviewed in Kinoshita, 2006; Versele and Thorner, 2005). Septins are phosphoproteins and are phosphorylated and de-phosphorylated throughout the cell cycle. Septins have been shown to be regulated by cyclin-dependent kinases, Cdc42 and its downstream effectors, and by phosphatases including PP2A. Cla4, a yeast orthologue of mammalian p21-activated kinases (PAKs), has been shown to directly phosphorylate septins and is downstream of Cdc42 activation (binds Cdc42-GTP through its CRIB domain). Cdc42 activation has been implicated in bud emergence and Cla4 most likely couples Cdc42 activation to changes in the septin complex, which results in

assembly of the septin collar. Historically, SUMOylation has been thought to be important for septin disassembly; however, recent results question those findings (Versele and Thorner, 2005).

In *S. cerevisiae*, septins act as both scaffolds for recruiting key molecules required for cell division and as diffusion barriers to direct polarized bud growth and to confine molecules required for division in the area around mother-bud neck. Although septins have been shown to be recruited to the cleavage furrow in mammalian cells as well (Schmidt and Nichols, 2004), they are also highly expressed in non-dividing cells (for example, the central nervous system), suggesting a role for septins in other cellular processes.

Septins in mammalian cells

In mammalian cells, septins have been shown to interact with both actin filaments and microtubules and are important for several cellular processes, including cell division (discussed in detail in the next section), vesicle trafficking and remodeling of the cytoskeleton. Determining the role of septins in mammalian cells has been difficult due to apparent redundancies in septin monomers and the presence of multiple isoforms from the same septin locus. Although the human genome contains at least 13 known septin genes, additional complexity is added through differential splicing to generate multiple isoforms of specific septin monomers. For example, the Septin 9 locus is particularly complex with at least 18 known transcripts producing 15 distinct Septin 9 isoforms (Scott et al., 2005). The shuffling of six different 5' and three different 3' splice variants leads

to this complexity. While alternative splicing has been seen in other septin loci, it is entirely possible that all septin isoforms have not been identified. Finally, expression profiling of human septins has shown that while some septin isoforms are highly expressed in distinct tissues, others show broader expression profiles (Hall et al., 2005). This added complexity has made interpreting results more difficult.

The stability of actin filaments and septin filaments appears to be codependent in mammalian cells (Kinoshita et al., 2002). In fibroblasts, Kinoshita et al. observed septins in a linear organization along actin filaments. Disruption of the actin network with cytochalasin D resulted in the formation of septin rings in the cytoplasm. These rings are similar to those observed when septin complexes are allowed to form *in vitro* and might represent a default or storage state of septins *in vivo*. Conversely, disruption of septins in fibroblasts using siRNA resulted in the reduction of actin filaments. Therefore, there is a reciprocal link between the stability of actin and septin filaments *in vivo*. *In vitro* studies have shown that the binding of septins to actin filaments is indirect and requires adaptor proteins.

Anillin, a contractile ring protein, is one such adaptor that can bundle actin filaments and recruit septin complexes to these bundles (Kinoshita et al., 2002). In addition, anillin binds non-muscle myosin II and may link septins to the actomyosin ring during cytokinesis. Finally, anillin contains a PH domain for targeting to the plasma membrane; mutation of this domain in the fly homolog of anillin resulted in defective targeting of septins during cytokinesis (Field et al., 2005). In fibroblasts, over-expression of a

fragment of anillin that can bind septins but not actin filaments resulted in loss of both septin and actin filaments (Kinoshita et al., 2002). Therefore, although septins do not directly bind actin filaments, they are required to stabilize these filaments *in vivo*. Since anillin is restricted to the nucleus until the nuclear membrane is dissolved during division, other adaptors must also be present that link septin and actin filaments, as anillin and septins only colocalize during cell division.

Like their yeast counterparts, it is assumed that mammalian septins are regulated by phosphorylation and recombinant septins have been shown to be phosphorylated *in vitro* (reviewed in Kinoshita, 2006); however, in mammalian cells the importance of phosphorylation or the kinases involved are still largely unknown. Mammalian septins have been shown to interact with different signaling molecules including the Borg family of proteins, which are downstream effectors of Cdc42 (Sheffield et al., 2003). Borg proteins contain a CRIB domain for binding activated Cdc42 and a BD3 domain for interacting with septin complexes. Borg3 interacts with the coiled-coil regions of the Sept6/7 heterodimer and the Sept2/6/7 trimer, but not with individual septin monomers. These data have led to the hypothesis that Borg3 interacts with the interface of the Sept6/7 heterodimer. Over-expression of Borg3 or more specifically the BD3 domain in MDCK cells resulted in aggregation of septin filaments (Joberty et al., 2001). This activity is blocked by activated Cdc42, which inhibits Borg3 from binding to septin complexes.

Expression of constitutively active Rho or its downstream effector Rhotekin also results in disruption of septin filaments in fibroblasts (Ito et al., 2005). The interaction of Rhotekin with septin complexes most likely involves indirect binding to the septin unique element of Sept9. Interestingly, using a yeast two-hybrid screen, Sept9 was also shown to interact with a RhoGEF, which was termed SA-RhoGEF (for septin-associated) (Nagata and Inagaki, 2005). Binding of Sept9 to SA-RhoGEF blocked SA-RhoGEF activation of Rho. This interaction required the N-terminal variable region of Sept9. Therefore, it is possible for Sept9 to bind both Rhotekin and SA-RhoGEF through distinct domains and provide a feedback loop for Rho signaling (reviewed in Spiliotis and Nelson, 2006). It should be noted that, although only one isoform of Sept9 was examined in these studies, Sept9-alpha (also known as Sept9_v3 or previously known as Sept9b), the ability of different isoforms to bind SA-RhoGEF may be important in tumor progression (discussed below).

Finally, septins have been proposed to act as diffusion barriers in mammalian cells as well. Two groups working independently discovered that Sept4 is essential for reproduction in humans and mice (Ihara et al., 2005; Kissel et al., 2005). Sept4 KO males are sterile due to defects in sperm morphology and motility. The mammalian sperm tail is segregated by a proposed plasma membrane diffusion barrier termed the annulus. It was discovered that the annulus is actually a septin ring and disruption of Sept4 results in loss of this structure, yielding sperm with defects in flagellar motility and structural integrity. Sept4 KO sperm are considerably more fragile than wild-type sperm, and have breaks or bends at several distinct regions in the sperm tail. Interestingly, the entire septin complex

is disrupted in Sept4 KO sperm, as the remaining septins are mis-localized throughout the cytoplasm in the absence of Sept4 (the remaining septins were only slightly reduced at the protein level). In humans, the loss of the septin ring has been shown as one of the causes of asthenospermia or infertility due to immotile sperm in sterile men.

Role of septins in mammalian cell division

Septins are clearly essential for cell division in budding yeast, so it is not surprising that cell cycle defects have been observed in various mammalian systems when septin complexes are disrupted (although the penetrance is not as high) (Nagata et al., 2003; Spiliotis et al., 2005; Surka et al., 2002). During mitosis, septins have been shown to co-localize with both actin filaments in the cleavage furrow and with microtubules at the central spindle in the cell mid-body. Although not definitively shown, based on the data from budding yeast, it is proposed that septin complexes act as a diffusion barrier at the cleavage furrow in mammalian cells as well (Schmidt and Nichols, 2004).

Septins have been shown to play key roles in regulating stability of microtubules and in the recruitment of proteins required for cell division. In HeLa cells, siRNA targeting of Sept7 (which also reduces Sept2 and Sept6) resulted in cells with multiple nuclei (~30% penetrant) (Kremer et al., 2005). This phenotype required the microtubule-associated protein, MAP4, as the mitotic defects were suppressed when MAP4 was knocked-down as well. MAP4 binds and bundles microtubules and prevents depolymerization. In this system, the septin complex directly bound MAP4 and prevented it from binding to

microtubules. In the absence of septins, microtubules were stabilized by MAP4 and the cells could not divide normally.

Division defects have also been observed when Sept9 was knocked-down in HeLa cells (similar observations were seen in epithelial cells) (Nagata et al., 2003; Surka et al., 2002). For these various systems, the gross phenotype of multi-nucleated cells is only observed in 10-20% of the treated populations. In HeLa cells, different isoforms of Sept9 co-localized with either actin filaments or with microtubules (Surka et al., 2002). Disruption of these interactions by injection of an anti-Sept9 antibody or by siRNA knock-down of Sept9 resulted in various mitotic defects, including multi-nucleated cells. In these cells, defects in abscission resulted in cells with an intact mid-body. This defect is similar to the one observed in yeast when either the septin or exocyst complex is disrupted (Dobbelaere and Barral, 2004). In addition, septins have been shown to co-immunoprecipitate with both the exocyst complex (Sec6/8) and with SNARE proteins in mammalian cells (reviewed in Joo et al., 2005), both of which are required for vesicle docking and fusion. These data support a role for septins in vesicle trafficking in mammalian cells and that Sept9 may function as a scaffold to target vesicle delivery to the site of abscission for membrane resolution.

Finally, division defects were also observed when Sept2 was knocked-down in epithelial cells (Spiliotis et al., 2005). In Sept2 siRNA treated epithelial cells, prometaphase is prolonged and various mitotic defects involved in chromosomal sorting were observed. Interestingly, the centromere-associated protein E (CENP-E), a mitotic motor and

checkpoint protein, was mis-localized in prometaphase. This led to the hypothesis that septins act as a mitotic scaffold to coordinate cytokinesis. From these experiments, it is clear that septins have diverse functions in cell division in both mammalian cells and in budding yeast, and that some of these functions may be conserved throughout evolution.

Septins in cancer and disease

Division defects that result in multi-nucleated cells can lead to mutations and aneuploidy, both of which can cause mis-regulated growth and, hence, tumor formation. Although links between aberrations in septin expression and cancer have been observed, the molecular details of how (or whether) septins function in tumors has not been definitively established. One of the first pieces of evidence suggesting that septins play a role in tumors came from patients with mixed-lineage leukemia (MLL) (reviewed in Russell and Hall, 2005). In a subset of these patients, chromosomal translocations leading to in-frame fusions of septin monomers with the proto-oncogene MLL were observed. MLL is a histone methyltransferase and a rather promiscuous oncogene with over 50 identified partners. Traditionally, MLL fusion proteins fall into two categories: proteins with transactivation domains or proteins that can oligomerize. To date, four septins (Septins 5, 6, 9 and 11) have been identified as fusion partners for MLL. In all cases, almost the entire reading frame of the septin monomer was part of the fusion and it has been hypothesized that these septins most likely function to oligomerize MLL (reviewed in Hall and Russell, 2004; Russell and Hall, 2005).

The first septin to be identified as an MLL fusion was Sept9 (reviewed in Russell and Hall, 2005). Interestingly, Sept9 has been implicated in several other cancers as well. Before the septin nomenclature was unified (Macara et al., 2002), Sept9 had various names, some of which were linked to different tumors. Sept9 was originally named MSF for MLL septin-like fusion (Osaka et al., 1999); it has also been named Sint 1 (Sorensen et al., 2000) and Ov/Br Septin (Russell et al., 2000). In mice, the Sept9 locus was shown to be an integration site for the SL3-3 retrovirus that induced T cell lymphomas (hence the name Sint 1 for SL3-3 integration site 1). Finally, in humans, the Sept9 locus has been identified as a region of allelic imbalance (loss or gain of an allele) in sporadic ovarian and breast cancers (hence the name Ov/Br Septin).

Mutations in the open reading frame of Sept9 have not been observed. This has led to the hypothesis that expression levels of septin monomers or specific isoforms of septin monomers may be more important for cancer than point mutations in the coding sequence (reviewed in Hall and Russell, 2004; Russell and Hall, 2005). Expression profiling of Sept9 isoforms in various healthy and diseased tissues supports this hypothesis (Robertson et al., 2004). A unique isoform of Septin 9 (Septin 9 zeta or Septin9_v4*) is only found in tumors. This isoform has the same coding sequence as the beta isoform of Septin 9 (Septin9_v4) but differs in the 5' untranslated region. This alteration may lead to differences in the rates of translation or in mRNA stability. Interestingly, over-expression of this Septin 9 isoform in epithelial cells resulted in increased actin protrusions and cell motility in wound-healing assays (Chacko et al., 2005). As mentioned above, Sept9 inhibits Rho activation induced by SA-RhoGEF (Nagata and Inagaki, 2005); however,

the beta/zeta isoforms of Septin 9 lack the required binding domain to interact with SA-RhoGEF. Therefore, over-expression of this isoform may result in over-activation of Rho signaling pathways, leading to increased cell migration (reviewed in Russell and Hall, 2005). Finally, in addition to altered expression in tumors, septins are mis-regulated in neurological disorders such as Parkinson's and Alzheimer's disease (Hall et al., 2005). Clearly, further understanding of the roles of septins in these different disorders may provide meaningful insights into future treatments for these devastating diseases.

Conclusion

Septins are regarded as scaffold proteins in both yeast and mammalian cells. Varying the levels of these proteins could have profound effects on several different cellular processes, including the stability of actin filaments and microtubules (reviewed in Russell and Hall, 2005). In addition, reducing the levels of specific septin monomers results in the reduction of other members of the septin complex. The role of septins in lymphocytes and highly motile cells has not been investigated, even though several septins are highly expressed in lymphoid tissues (Hall et al., 2005). Therefore, we decided to study the role of septin complexes in T cells.

**Figure 1** Structure of septin monomers and organization of heteromeric septin complexes. (**a**) Primary structure of septin monomers. All septins contain a core domain that consists of a GTP-binding domain, a septin-unique element and a polybasic region for binding phospholipids. Outside the core domain, septins have variable N-terminal and C-terminal extensions important for protein-protein interactions. Septins are classified into three distinct groups based on the homology of their c-terminal variable regions. The majority of septins contain a coiled-coil (CC) domain at their C-terminus. Members of the Sept2 group (Septins 1, 2, 4, 5, 7 and 13) have shorter CC regions than members of the Septin 6 group (Septins 6, 8, 10 and 11). Members of the Septin 3 group (Septins 3, 9 and 12) do not contain CC domains in their C-terminus. Septins 4, 8 and 9 also have a proline-rich domain (PRD) at their N-terminus. (**b**) Septins form heteromeric complexes that consist of multiple septin monomers. Sept7 is thought to be central to the septin complex and interacts with members of the Sept2 and Sept6 groups through their C-terminal CC domains. Members of the Sept3 group, which lack C-terminal CC domains, interact with the complex through their N-terminal variable regions which, at least for Sept9, contains a PRD. Adapted from Hall and Russell, 2004; Spiliotis and Nelson, 2006; and Versele and Thorner, 2005.

a

b

30
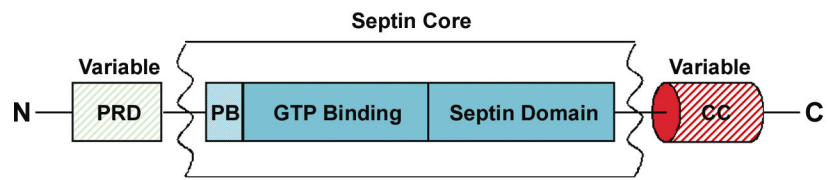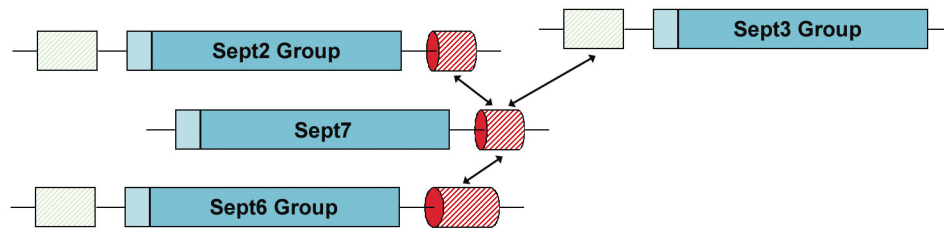
Chapter 3:

Annular and Cortical Septins Act as Structural Scaffolds to Maintain Shape and Limit Protrusions in T Lymphocytes

Summary

T cells exhibit a directional axis of polarity that is characterized by a well-defined anterior leading edge and a posterior protrusion called the uropod. We found that septins, cortical cytoskeletal polymers, are enriched as an annular 'collar' at the T cell mid-body. Depletion of septins resulted in both a pronounced increase in uropod length and the presence of bent uropods. Septin deficient T cells also exhibited structural instabilities resulting in membrane blebbing and the inability to control protrusions; however, only minor defects were observed in crawling velocity. Although myosin II activity was still required for uropod formation in septin deficient T cells, phosphorylation of myosin II heavy and light chains was not dysregulated. Finally, loss of septins did not affect functions that require cell polarization; however, septin deficient T cells rapidly permeated extremely small pores, consistent with the loss of a structural scaffold. We therefore conclude that cortical septins enriched at the T cell mid-body serve primarily as a lattice and are critical for structural integrity and limiting anterior and posterior protrusions.

Introduction

An important feature of T lymphocytes is their ability to migrate through tissues in search of antigen presenting cells (APC) bearing peptide-MHC complexes. The highly polarized morphology of T cells is required for efficient migration within lymph nodes and peripheral tissues as well as for their reactivity to antigen-bearing APC (Sanchez-Madrid and del Pozo, 1999). In this mode, T cells utilize an amoeboid form of migration characterized by actin polymerization at the leading edge 'pseudopod,' followed by contraction in the cytoplasmic-rich uropod.

Septins were first identified in yeast by temperature-sensitive mutants that resulted in cell division defects (Koshland et al., 1985) and are localized at the mother-bud neck during cell division (reviewed in Kinoshita, 2006; Versele and Thorner, 2005). Individual septins assemble as hetero-oligomers to form filaments, rings and gauzes (Rodal et al., 2005) which act as molecular scaffolds and, in some settings such as the cytokinetic furrow, function as a diffusion barrier to maintain cell fate determinants in the appropriate cell (Dobbelaere and Barral, 2004; Takizawa et al., 2000). Similar septin rings are found in mammalian cells undergoing division (Schmidt and Nichols, 2004) and loss of these structures in mammalian cells can also result in defective cytokinesis (Kremer et al., 2005; Spiliotis et al., 2005; Surka et al., 2002).

Results and discussion

We first identified T cell expression of Sept9 in a gene-trap screen (Tooley et al., 2005) for molecules involved in polarity (data not shown). Subsequent analysis of septin expression

in a murine T cell line (Supplemental Figure 1) by reverse transcriptase-PCR indicated

significant expression of Septins 1, 2, 6, 7, 8, 9, 10, 11. This pattern of RNA expression is

consistent with expression profiling of human septins (Hall et al., 2005). In order to assess

the relevant protein levels in T cells, we used a panel of anti-septin specific polyclonal

antibodies. As shown in Figure 1a, we found significant expression of Septins 1, 6, 7, 8,

and 9. We were not able to assess the expression of Sept10 due to the absence of suitable

reagents and all other septins were not present above our level of detection (data not

shown). As has been previously described, both Sept8 and Sept9 are present in at least two

isoforms in T cells (Hall et al., 2005; Scott et al., 2005). As septins are known to

oligomerize and form heteromeric complexes (Kinoshita et al., 2002; Kremer et al., 2005;

Nagata et al., 2004; Surka et al., 2002) we assessed the presence of septin complexes in

lysates from D10 T cells. As shown in Figure 1b, immunoprecipitation of Septins 1, 6, 7 or

9 resulted in the co-precipitation of septin complexes containing every septin we have

identified in these cells.

Four of these antibodies proved suitable for immunofluorescent studies in T lymphocytes.

As shown in Figure 1c, these all had similar patterns, grossly highlighting the cell cortex in

crawling T cells with a frequent and significant enrichment through the mid-body, forming

an annular septin 'collar'. This distinctive pattern was most prevalent for Septins 7 and 9

and less so for Septins 1 and 6. However, all cells stained had significant septin staining in

this region, even when it was also present elsewhere on the cortex at similar high levels (for

example for Sept1 and Sept6). Higher resolution confocal imaging also revealed strand-

like patterns in a ring around the mid-body and into the uropod (Supplemental Figure 2 and

Supplemental Movie SM1) suggesting this 'collar' is indeed a series of arrayed strands. Weaker staining was also occasionally observed along the leading edge and more rarely inside the cell near the MTOC (most notable for Sept9, data not shown). Since these are not cells undergoing division, it seemed possible that septins play a role in polarity, such as creating a diffusion barrier for front-to-back determinants, or in regulating the shape and integrity of the mid-body/uropod.

In order to assess the functional requirements for septins in T cells, we specifically targeted Septins 1, 6, 7 and 9 using plasmid-based short hairpin RNAs (shRNAs). As shown in Figure 2a, we achieved significant knock-down (KD) of Septins 1,6,7, and 9 in D10 T cells when each was specifically targeted. In addition, targeting of Sept7 resulted in the reduction of the entire septin complex (Figure 2a, b), a result that was specific to Sept7, as the reciprocal was not observed when other septins were targeted. This supports the hypothesis that Sept7 is central to the septin complex and may act as a core to which other septins are added (Kinoshita et al., 2002; Kremer et al., 2005; Nagata et al., 2004).

We subsequently generated a second shRNA targeting Sept7 (KD #2) at a distinct site in order to confirm that our results were specific to Sept7 KD and expression of either shRNA resulted in similar reductions in all septins observed (Figure 2b). We were able to reproducibly achieve greater than 80% KD of Septins 6,7,8, and 9 and over 70% of Sept1 using these two shRNAs. Although septin knockdown leads to defects in cell division in other systems (Nagata et al., 2003; Spiliotis et al., 2005; Surka et al., 2002), Sept7 KD in

D10 T cells did not show any defects in cell division for at least the first 72 hour period during which our further observations were made (Supplemental Figure 3).

Septin staining in crawling D10 T cells is enriched at the mid-body, a region also enriched in myosin-IIA, the predominant class II myosin expressed in T cells. Disruption of myosin-IIA, either by treating the cells with the chemical inhibitor Blebbistatin (Straight et al., 2003) which blocks motor activity or by loss of the protein through shRNA targeting, resulted in T cell rounding (Jacobelli et al., 2004). If myosin II and septins were working together to regulate uropod formation, we would expect to see similar results in Sept7 KD T cells. However, as shown in Figure 2c and d, we observed the opposite phenotype as Sept7 KD T cells exhibited on average almost a two-fold increase in uropod length. The average uropod length in KD cells was 14.4 ± 4.3 μm for Sept7 KD#1 (n = 107) and 15.1 ± 3.7 μm for Sept7 KD #2 (n = 108) versus 8.8 ± 2.0 μm for control shRNA treated cells (n = 97). The standard deviation was also higher indicating a broader range of diversity in the KD populations, most likely resulting from various degrees of KD in individual D10 T cells. Furthermore, only the length of the uropod was increased in Sept7 KD T cells, as the length of the cell body was not altered (Figure 2e). This phenotype was not observed when Septins 1, 6 or 9 were targeted and was not dependent on adhesion as cells floating in suspension had the same phenotype (data not shown). This result implies that septins function to restrict the length of the uropod in polarized T cells and may oppose myosin II function in the T cell mid-body.

In addition to an increase in uropod length in Sept7 KD T cells, as shown in Figures 2c,d and f, we observed a significant abnormality whereby the uropod was visibly bent. This was observed in 32% of Sept7 KD#1 (n=107) and 34% of Sept7 KD#2 (n=108) cells versus 10% of control treated cells (n=97). The segmentation of the posterior tail into sections may be taken to imply that there are normally regional variations in the tail domain that are not resolved in wild-type T cells. Interestingly, sperm from Sept4 deficient mice have structural defects that also result in broken and kinked tails (Ihara et al., 2005; Kissel et al., 2005), suggesting a common function for septins in the middle of non-mitotic mammalian cells, particularly those with elongated morphologies. Finally, in budding yeast, disruption of septin complexes (Gladfelter et al., 2005) or molecules involve in septin assembly (Longtine et al., 1998) resulted in elongated buds with a narrow neck morphology, indicating septins regulate cell shape in other systems as well.

Defects due to septin disruption in T cells were not confined to the uropod. We also observed defects in structural integrity of the plasma membrane in Sept7 KD D10 T cells. While acquiring time-lapse images, we observed two types of membrane defects: membrane blebbing and the presence of excess protrusions (Figure 3a and Supplemental Movies SM2, SM3 and SM4). Membrane blebbing was dynamic and mainly confined to the cell body. As shown in Figure 3b, this phenotype was observed in 29.7% (KD #1, n = 118) and 37.1% (KD #2, n = 140) of Sept7 KD T cells versus 9.9% of the control treated population (n = 151). The same cells were scored for the presence of excess protrusions characterized by long, thin appendages that formed and were eventually re-absorbed. These protrusions emanated from both the leading edge and the cell mid-body (data not

shown). Although these protrusions were observed at a lower frequency than membrane blebbing (Figure 3b), there was a significant increase in the number of excess protrusions in both Sept7 KD T cells (KD #1 = 9.3%, KD #2 = 15.0%) compared to the control treated population (2.0%). For quantification, cells were scored if present for at least five minutes during the imaging period. Therefore, the percentage of cells with these types of structural defects may have been higher if the cells were monitored longer.

Despite these considerable morphological abnormalities, Sept7 KD T cells exhibited only minor defects in crawling velocities *in vitro*. Sept7 KD T cells crawled at 7.5 ± 1.9 μm/min (KD #1, n = 36) and 7.0 ± 1.8 μm/min (KD #2, n = 35) compared to 8.5 ± 2.6 μm/min for control treated cells (n = 30). This result was somewhat surprising and suggests little physical significance for the distal tip of the uropod in T cell crawling, since it is both elongated and, often at an angle to the direction of motility in these cells (see Supplemental Movie SM3). Such a conclusion is also supported by observations we have made using TIRF imaging that place the critical regions for amoeboid adhesion in the region forward of the uropod (J. Jacobelli and MF Krummel, unpublished observations). We speculate that the small differences in velocities observed *in vitro* might lead to greater differences *in vivo*, where cells migrate in a confined three-dimensional environment filled with other cells and in which an uncoordinated uropod might be a more substantial deficit.

As the phenotype of Sept7 KD is the opposite of myosin II inhibition, we sought to confirm that myosin activation was responsible for the elongation of the uropod, or,

conversely if other mechanisms were operating to lengthen this structure in the absence of septins. ROCK inhibition results in loss of the uropod (Lee et al., 2004), presumably due to decreased phosphorylation of myosin light chain. Treatment of KD and control cells with ROCK inhibitor Y-27632 resulted in a complete loss of the uropod (Figure 4a and Supplemental Movie SM5) showing that the elongated phenotype required active myosin II. Similarly, blocking myosin-IIA activity by treating the cells with Blebbistatin also resulted in complete loss of the uropod in KD and control cells (Figure 4b and Supplemental Movie SM6). Taken together, this data indicates that the Rho/ROCK signaling pathway is still required for uropod formation in the absence of septin complexes.

The subsequent result raised the possibility that septins repress myosin function in the mid-body. Regulation of myosin II involves phosphorylation of both the myosin light chains (MLC) and the myosin heavy chain (Myh9). Phosphorylation of the light chain results in increased motor activity and increased tension through bundling of actin filaments; conversely, phosphorylation of the heavy chain results in decreased tension through de-bundling of actin filaments (Dulyaninova et al., 2005; Jacobelli et al., 2004). Sept9 has also been shown to interact with Septin-Associated Rho-GEF (SA-RhoGEF) (Nagata and Inagaki, 2005), which might result in regulated Rho and therefore ROCK activation. Binding of Sept9 to SA-RhoGEF blocks SA-RhoGEF activation of Rho. As shown in Figures 4c and 4d, there were no detectable differences in the phosphorylation state of either MLC or Myh9 nor changes in the overall levels of myosin II (Figure 4d). We likewise did not observe any localized increase in myosin II or the phosphorylation of

light or heavy chains confined to the mid-body, as assessed by immunohistochemistry (data not shown).

Although no changes in myosin II were observed in Sept7 KD T cells, as shown in Figure 4e, we observed a 10% to 30% reduction in the levels of F-Actin as assessed by phalloidin staining. The levels of total actin were not changed in Sept 7 KD T cells (Figure 4c). Taken with the myosin data, this finding is most consistent with a myosin-independent role for septins in regulating actin stability, a result that has also been observed in other cell types (Kinoshita et al., 2002). It is not clear if the structural defects we observed in crawling and morphology (Figures 2 and 3) are from reduction in actin filaments, reduction in the septin cytoskeleton or a combination of both.

A potential consequence of the destabilization of the mid-body might be a loss of polarity, particularly if septins in the mid-body also act as a diffusion barrier at this site. A loss of overall polarity was not observed in Sept7 KD T cells, as the MTOC was correctly positioned behind the nucleus in crawling cells (Figure 5a). A loss of polarity in T cells consistently results in a loss of reactivity to antigen-bearing APCs, presumably due to a required segregation of signaling molecules toward or away from the immunological synapse. Thus, for example, loss of classical polarity regulators such as Dlg (Round et al., 2005) or Scribble (Ludford-Menting et al., 2005) or PKCz (Leitges et al., 2001) all result in significant inabilities of those cells to trigger via their TCR and form couples with APCs. In contrast, Sept7 KD T cells have antigen dose-dependent coupling efficiencies with APCs that are indistinguishable from control shRNA treated cells (Figure 5b).

Taken together this suggests that critical anterior-posterior segregation remains intact in the absence of septin complexes.

Although Sept7 KD T cells show no gross defects in crawling velocity, we suspected that the elongation and/or loss of structural integrity would alter their ability to transmigrate in response to chemotactic stimuli. Although the specific chemotaxis for the D10 cell line to MIP-1a is typically low, both control and Sept7 KD T cells responded to chemokine gradients. No increase in specific chemotaxis was observed when chemokine was added to the top chamber as well (data not shown). However, the modest chemotaxis of Sept7 KD T cells occurred against a two-fold increase in the basal transmigration of these cells through 8 μm pores in the absence of chemokine. Since overall speed is not significantly altered in Sept 7 KD T cells (Figure 3c), we hypothesized that these cells were able to pass through 8 μm pores more efficiently than control cells.

To test this hypothesis, we examined transmigration of Sept7 KD T cells using transwells with smaller (3 μm and 5μm) pores in the absence of chemokine. Control treated D10 T cells were essentially unable to pass through both 3 μm and 5 μm pores (2.0% and 3.7% transmigration, respectively). However, Sept7 KD D10 T cells transmigrated through both 3 μm and 5 μm pores approximately five-fold better than control cells (at 10.7% and 15.7% transmigration, respectively for Sept7 KD#1 and 8.8% and 14.1% transmigration, respectively for Sept7 KD#2).

This final result indicates that septin complexes act as a structural scaffold to negatively regulate T cell transmigration and may have implications for *in vivo* transmigration and/or tumor metastasis. When lymphocytes exit the bloodstream, they must squeeze through high-endothelial venules, an event that may be regulated by septin complex modulation or may simply be regulated by cell rigidity and girth, a parameter normally set by the septin cytoskeleton. Septin expression is altered in various human and mouse tumors (Hall et al., 2005; Hall and Russell, 2004; Russell and Hall, 2005) and ensuing alterations in cell morphology and specific aspects of motility may provide a possible mechanism to enhance tumor metastasis and progression.

Methods

Cell Culture. The D10.G4 CD4+ T cell clone was used in all experiments and was maintained in RPMI 1640 supplemented with 10% FCS, L-glutamine, penicillin, streptomycin, β-mercaptoethanol and 50 U/ml interleukin-2 (IL-2) as described (Jacobelli et al., 2004). Cells were re-stimulated weekly with conalbumin (134-146) peptide-pulsed irradiated splenocytes from B10.Br donor mice. All mice were bred and maintained in accordance with the guidelines of the Lab Animal Resource Center of the University of California at San Francisco.

Antibodies and reagents. The following antibodies were used for cell staining and immunoblotting: anti-septin antibodies were provided by M. Kinoshita and WT Trimble; anti-phospho-MLC2 (Ser19) mouse monoclonal #3675 (Cell Signaling); anti-actin, clone C4 (Chemicon); anti-α-tubulin clone B-5-1-2 (Sigma); anti-pThr1939-Myh9, a rabbit polyclonal was made against a c-terminal phosphopeptide of Myh9 (Jacobelli et al., 2004); rabbit anti-class II myosin polyclonal (BTI); rabbit polyclonal anti-pericentrin (Covance); and APC-conjugated anti-CD19 clone 1D3 (BD Pharmingen).

Rhodamine- and FITC-conjugated donkey anti-rabbit secondary reagents were purchased from Jackson ImmunoResearch Laboratories. Horseradish-peroxidase-conjugated goat anti-mouse and Protein-A, and detergent compatible protein assay kit were purchased from Bio-Rad. Hoechst 33342 was used for nuclear staining of live cells and Alexa Fluor 647-conjugated phalloidin were purchased from Invitrogen. Protease inhibitors: aprotinin, phenylmethylsulfonyl fluoride (PMSF), sodium fluoride, iodoacetamide and sodium

orthovanadate were purchased from Sigma. Protein-A sepharose was purchased from GE Healthcare. Y-27632 and Blebbistatin were purchased from Calbiochem. Recombinant murine MIP-1α (CCL3) was purchased from PeproTech and Corning 3, 5 and 8 μm transwells were purchased from Fisher Scientific.

RNA isolation and reverse transcriptase PCR. RNA was isolated from D10 T cells and whole tissue extracts of mouse spleen and brain using the TRI Reagent (Sigma). For septin expression screening, cDNA synthesis was carried out using Superscript III (Invitrogen), followed by 28 cycles of PCR using Stratagene's EasyA Polymerase. Primers used for septin screening are shown in Supplemental Table 1. Primers against Hypoxanthine-guanine phosphoribosyltransferase (HPRT) (5'– CTCGAAGTGTTGGATACAGGC – 3' and 5' – GATAAGCGACAATCTACCAGAG – 3') were used as a positive control to confirm cDNA synthesis was successful.

Lysis, immunoprecipitation and immunoblotting. D10 T cells were lysed in PBS containing 1% Triton X-100 in the presence of a cocktail of protease and phosphatase inhibitors (2 μg/ml aprotinin, 2 μg/ml leupeptin, 2 mM PMSF, 10 mM sodium fluoride, 10 mM iodoacetamide and 1 mM sodium orthovanadate). Equal amounts of cell lysates, as determined with the BioRad detergent-compatible protein assay, were then resolved by SDS-PAGE and immunoblotting analysis was performed using primary and secondary antibodies described above. For immunoprecipitations, both calcium and magnesium chloride (1 μm each) were added to the lysis buffer and septin complexes were

immunoprecipitated from D10 lysates for three hours at 4°C using Protein-A sepharose

beads. Lysates were pre-cleared with beads coated with normal rabbit serum.

Cell staining. Cells were incubated at 37°C on superfrost plus slides (VWR

International) for at least one hour before fixing with 1% PFA (supplemented with 1 mM

calcium and magnesium chloride) at 37°C for 10 min. For pericentrin staining, cells were

fixed with 1% PFA for five min followed by five min with cold methanol. Cells were

then centrifuged down onto the slides at 200xg for 5 min. Fixed cells were blocked with

2% donkey serum and permeabilized with 0.02% saponin (Sigma) in PBS for 30 min.

The primary antibodies were incubated for 60 min, then extensively washed and followed

by secondary antibody staining for 60 min. After thorough washing the cells were treated

with anti-fade reagent (BioRad) and the slides were sealed and imaged. For septin

staining, only morphologically polarized crawling T cells were scored for enrichment at

the T cell mid-body. All image analysis and measurements were done using Metamorph

software.

Plasmids and transfections. pSilencer 2.0 shRNA expression vector using the human

U6 promoter was purchased from Ambion. Primers for hairpins were ordered from IDT

and Sigma and cloned following manufacturers instructions. Two hairpins were designed

against Sept7 (KD #1, 5'-GGATTTGAATTCACTCTTA-3' and KD #2, 5'-

GGATCCGTTTGACCAATTT-3'), targeting the open reading frame and the 3'

untranslated region, respectively. Hairpins against Sept1 (5'-

GCCTGCCCTTGCACTTAAA-3'), Sept6 (5'-GCTTAAGTCTCTGGACCTAGT-3')

and Sept9 (5'-GCCTAAGCAAAGTGGTGAACA-3') were also used in this study. A

negative control vector containing an shRNA with only limited sequence homology to

any known sequence in the mouse genome (5'-ACTACCGTTGTTATAGGTG –'3) was

used a negative control in this study. Control and shRNA expressing plasmids were

introduced into T cells by electroporation (Bio-Rad) and co-transfection of an EGFP

expressing vector, pEGFP-N1 (Clontech), was used as a positive marker for transfection

and for cell sorting. For transfection, 25 μg of plasmid DNA in a >7:1 molar ratio of

shRNA expressing plasmid to GFP reporter was used to transfect 50 million cells in a 0.5

ml volume. GFP positive cells were sorted 48-72 hours post-transfection using a MoFlo

cell sorter (Dako Cytomation). Sorted GFP positive cells were used approximately 72

hours post-transfection in all knock-down experiments in this study.

Microscopy. Imaging experiments were done using a modified Zeiss Axiovert 200M

microscope with a plan-neofluor 40X objective (Carl Zeiss). The microscope was fitted

with dual excitation and emission filter wheels and a photometrics Coolsnap-HQ camera.

Image acquisition and analysis was performed using Metamorph imaging software

(Molecular Devices). To examine T cell motility *in vitro*, imaging was performed in

0.25% low-melting point agarose and time-lapse images were recorded at 5, 10 and 30

second intervals. For velocity measurements, Hoechst 33342 (1μg/ml) was added to the

imaging chamber to visualize the nucleus and time-lapse images were acquired at 30-

second intervals. Migration of the nucleus was then used to track the cell path for velocity

measurements. To examine membrane dynamics, time-lapse images were acquired at

higher frequencies (5 and 10 second intervals). For these experiments, Hoechst 33342 was not added to cells, as it appears to be toxic when illuminated too frequently.

Inhibitor studies. Cells were treated with either the ROCK inhibitor Y-27632 (10 μM final) or the myosin II inhibitor Blebbistatin (racemic, 100 μM final). For Y-27632, the drug was added five frames after the start of imaging, while for Blebbistatin, imaging was started immediately after addition of the drug. For inhibitor studies, 0.1% low-melting point agarose was used for both inhibitors, as the drugs did not diffuse well in 0.25% agarose. DMSO controls did not alter the morphology or crawling of control or shRNA treated cells.
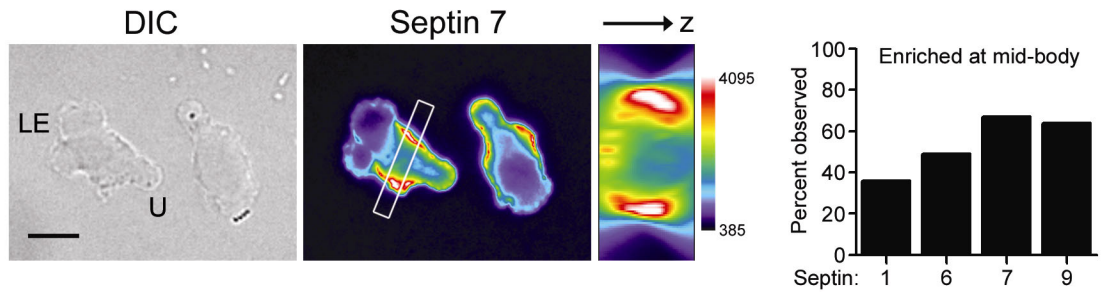
F-Actin quantification. Cells were fixed immediately after removing from 37°C to maintain cell morphology. T cells were permeabilized and stained using 3 units of Alexa Fluor 647-conjugated phalloidin according to the manufacturer's protocol. F-Actin staining was quantified using a BD FacsCalibur and data was analyzed using FloJo.

Coupling assay. Control or Sept7 KD D10 T cells and CA-pulsed CH27 B cells were mixed together, briefly centrifuged at 200xg and incubated at 37º C for 45 min. Cells were then fixed with 1% PFA for 10 min at RT, washed and the B cells were stained with APC-conjugated anti-CD19 (T cells were not stained as they were already GFP-positive). Cells were then analyzed using a BD FacsCalibur flow cytometer and CellQuest Facs analysis software. Percent coupling was quantified as the number of T cells in double-

positive quadrant (GFP- and CD19-positive) versus the total numbers of T cells (GFP-positive).

Chemotaxis and transmigration assay. Chemotaxis assays were carried out using transwells with 8 μm pores, as the D10 T cell line used in this study does not efficiently transmigrate through 5 μm pores. MIP-1α (used at 1 μg/ml) was added to the bottom well of the transwell chamber and used as a chemotactic stimuli. For transmigration assays, 3 μm and 5 μm pores were used in the absence of chemokine. Chemotaxis and transmigration assays were performed at 37°C for 4 hours in the absence of FCS, before cells were harvested and counted for a fixed amount of time on a BD FacsCalibur flow cytometer. Data was analyzed using CellQuest Facs analysis software.

Figure 1 Septin complexes form in T cells and assemble as a 'collar' in the mid-body. (**a**) D10 T cells express Septins 1, 6, 7, 8 and 9. A panel of anti-septin specific polyclonal antibodies was used to screen lysate from D10 T cells in order to determine the septins that are expressed at the protein level. D10 T cells express at least two isoforms of Sept8 and Sept9. (**b**) Septins form heteromeric complexes in D10 T cells. Septins 1, 6, 7 or 9 were immunoprecipitated from D10 lysate and blotted for the remaining septins shown to be expressed in (**a**). Normal rabbit serum was used to pre-clear (PC) the lysate and as a control for immunoprecipitation (C). The band present in all samples in the Sept9 blot corresponds to the heavy chain (HC) of the antibody used for the immunoprecipitation. (**c**) Septins localize to the cell cortex in crawling D10 T cells. Crawling D10 T cells were fixed and stained for Septins 1, 6, 7 and 9 (anti-Sept8 antibodies did not reproducibly stain fixed cells). In addition to staining at the cell cortex, Sept7 (67%, n = 67) and Sept9 (64%, n = 64) were enriched at the T cell mid-body or neck. This enrichment was less evident for Sept1 and Sept6, for which a clear 'collar' phenotype could only be defined in 36% (n = 66) and 49% (n=68) of the cells, respectively. A three-dimensional reconstruction of a transverse section (indicated by the white box), demonstrating the presence of an annular septin collar at the T cell mid-body. Bar, 10 μm, LE = leading edge, U = uropod. Pooled totals from three independent experiments.

a

Septin: 1   6   7   8   9

160 —
105 —
75 —   ——α,ε,γ
50 —
                ——δ
35 —

b

Septin

IP: PC C   1   6   7   9

Septin 1

Septin 6

Septin 7

Septin 8

Septin 9

HC

c

DIC   Septin 7   → z

LE

U

4095

385

Enriched at mid-body

Percent observed

100
80
60
40
20
0

Septin: 1   6   7   9
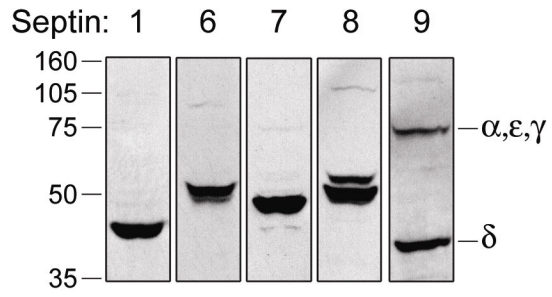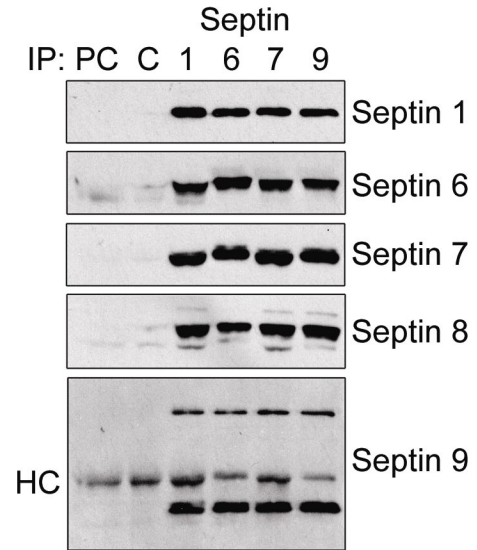
Figure 2 Sept7 knock-down (KD) in T cells and resulting defects in T cell morphology.

(**a**) shRNAs were designed against Septins 1, 6, 7 and 9 and transfected into D10 T cells.

Individual targeting of Septins 1,6,7 and 9 resulted in specific KD of these proteins. In

addition, KD of Sept7 results in the loss of all other known septins, indicating Sept7 is

required for stability of septin complexes in T cells. Reduction of other septins was only

observed when Sept7 was targeted. Protein levels were examined by Western blotting 72

hours post-transfection. Lysates from septin KD T cells were compared against cells

treated with a negative control shRNA (C = control). For Sept9, only the predominant

40kD isoform is shown; however, the larger isoforms are reduced as well (data not

shown). This result confirms the specificity of the antibodies used throughout this study.

(**b**) Reduction in septin complexes is specific to Sept7. We generated a second shRNA at

a distinct location in order to confirm the results were specific to targeting Sept7. Tubulin

blots shown in (**a**) and (**b**) are representative as samples were run on multiple gels. (**c**)

Sept7 KD D10 T cells have morphological defects as exhibited by an increase in uropod

length. Hoechst 33342 was used to distinguish the nucleus (highlighted in blue) from the

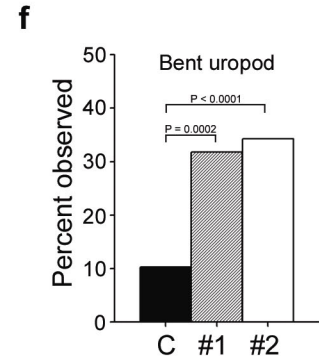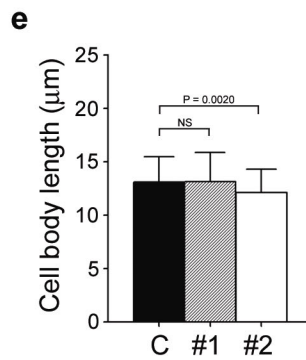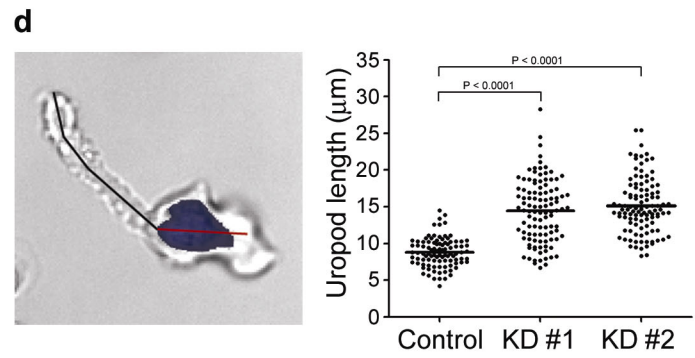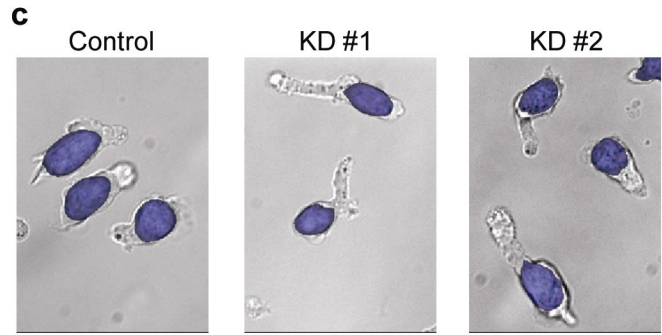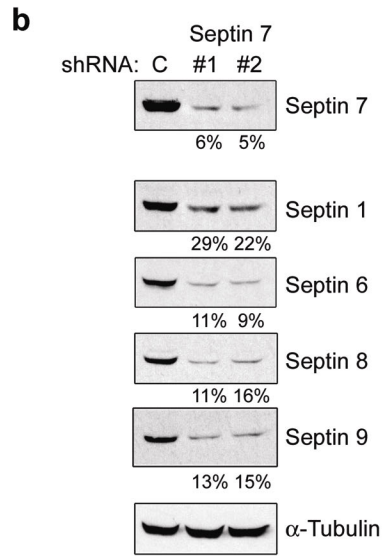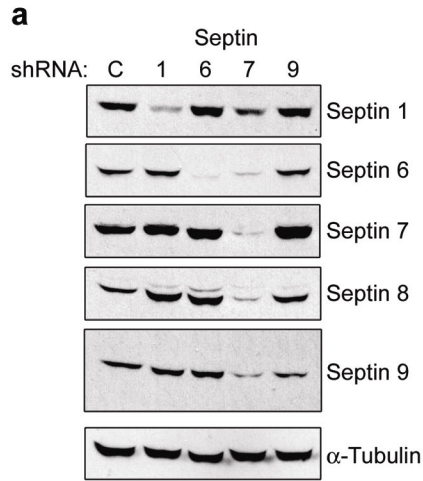cytoplasm. (**d**) Sept7 KD T cells have on average almost a two-fold increase in uropod

length. In order to quantify the increase in uropod length, a line was drawn from the end

of the uropod to the nucleus (black line). The average uropod length in Sept7 KD cells

was 14.4 ± 4.3 μm for Sept7 KD#1 (n = 107) and 15.1 ± 3.7 μm for Sept7 KD #2 (n =

108) versus 8.8 ± 2.0 μm for control shRNA treated cells (n = 97). (**e**) Only the length of

the uropod was increased in Sept7 KD T cells, as the length of the cell body (red line in **d**)

was not dramatically altered. (**f**) In addition to being longer, Sept7 KD T cells exhibited

bent uropods indicating structural problems in the absence of septin complexes. A uropod

was scored as bent if a straight line traveling through the cell from the distal tip of the

uropod to the beginning of the nucleus could not be drawn. These defects were observed

in 31.8% (KD #1, n = 107) and 34.3% (KD #2, n = 108) of Sept7 KD T cells versus

10.3% of control cells (n = 97). (**d**, **e**) Representative mean ± s.d. pooled from three

independent experiments. Statistical analysis performed using an unpaired *t* test (**e**) with

Welch's correction for unequal variance (**d**). (**f**) Pooled total from three independent

experiments, statistical analysis performed using the chi-squared test.

a

Septin

shRNA: C   1   6   7   9

Septin 1
Septin 6
Septin 7
Septin 8
Septin 9
α-Tubulin

b

Septin 7

shRNA: C   #1   #2

Septin 7
6%   5%

Septin 1
29% 22%

Septin 6
11% 9%

Septin 8
11% 16%

Septin 9
13% 15%

α-Tubulin

c

Control   KD #1   KD #2

d

P < 0.0001
P < 0.0001

Uropod length (μm)

Control   KD #1   KD #2

e

Cell body length (μm)

P = 0.0020
NS

C   #1   #2

f

Bent uropod

P < 0.0001
P = 0.0002

Percent observed

C   #1   #2

53

Figure 3 Septins are required for structural stability of the cell cortex and at the T cell mid-body. (**a**) Sept7 KD T cells have structural defects resulting in membrane blebbing and excess membrane protrusions (also see Supplementary movies SM2, SM3 and SM4). Membrane blebbing was dynamic and mainly confined to the cell body. Excess protrusions emanated from both the leading edge and the T cell mid-body and persisted as long, thin membrane appendages. (**b**) Quantification of structural defects observed in Sept7 KD T cells. Membrane blebbing was observed in 29.7% (KD #1, n =118) and 37.1% (KD #2, n = 140) of Sept7 KD T cells versus 9.9% of the control treated population (n = 151). Excess protrusions were observed in the same population of cells, 9.3% and 15.0% for Sept7 KD#1 and KD#2, respectively, versus 2.0% for the control treated population. Pooled totals from three independent experiments. Statistical analysis performed using the chi-squared test. (**c**) Overall crawling velocity is not affected by Sept7 KD. Sept7 KD T cells crawled at 7.5 ± 1.9 µm/min (KD #1, n = 36) and 7.0 ± 1.8 µm/min (KD #2, n = 35) compared to 8.5 ± 2.6 µm/min for control treated cells (n = 30). Similar results were obtained in three independent experiments. Representative mean $\pm$ s.d. Statistical analysis performed using an unpaired *t* test.
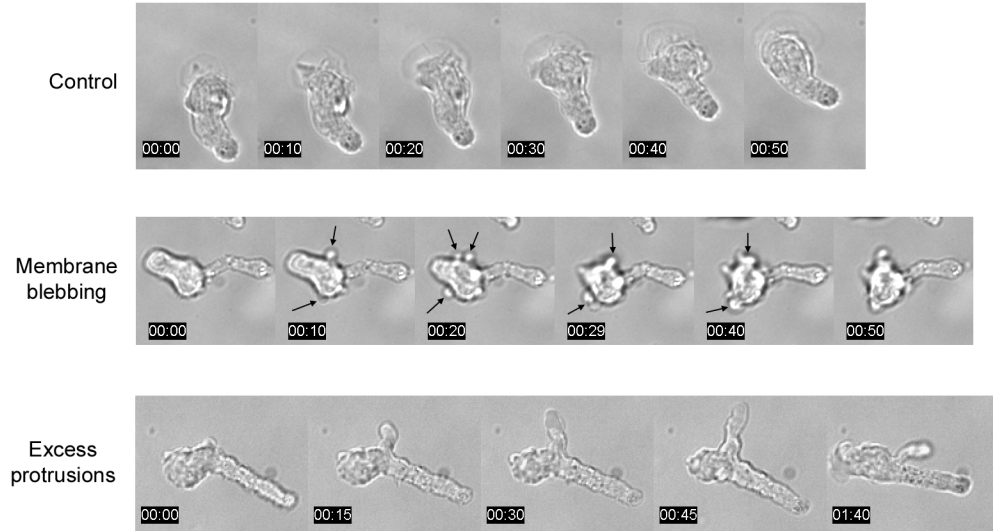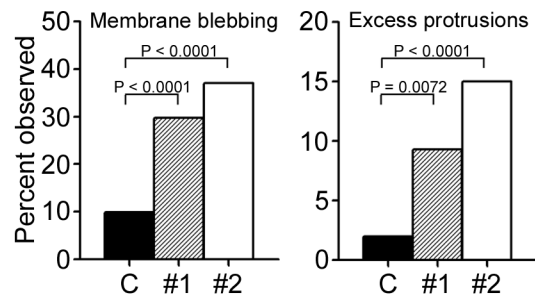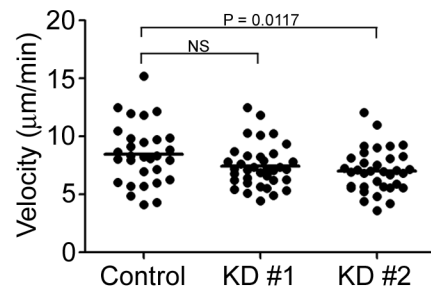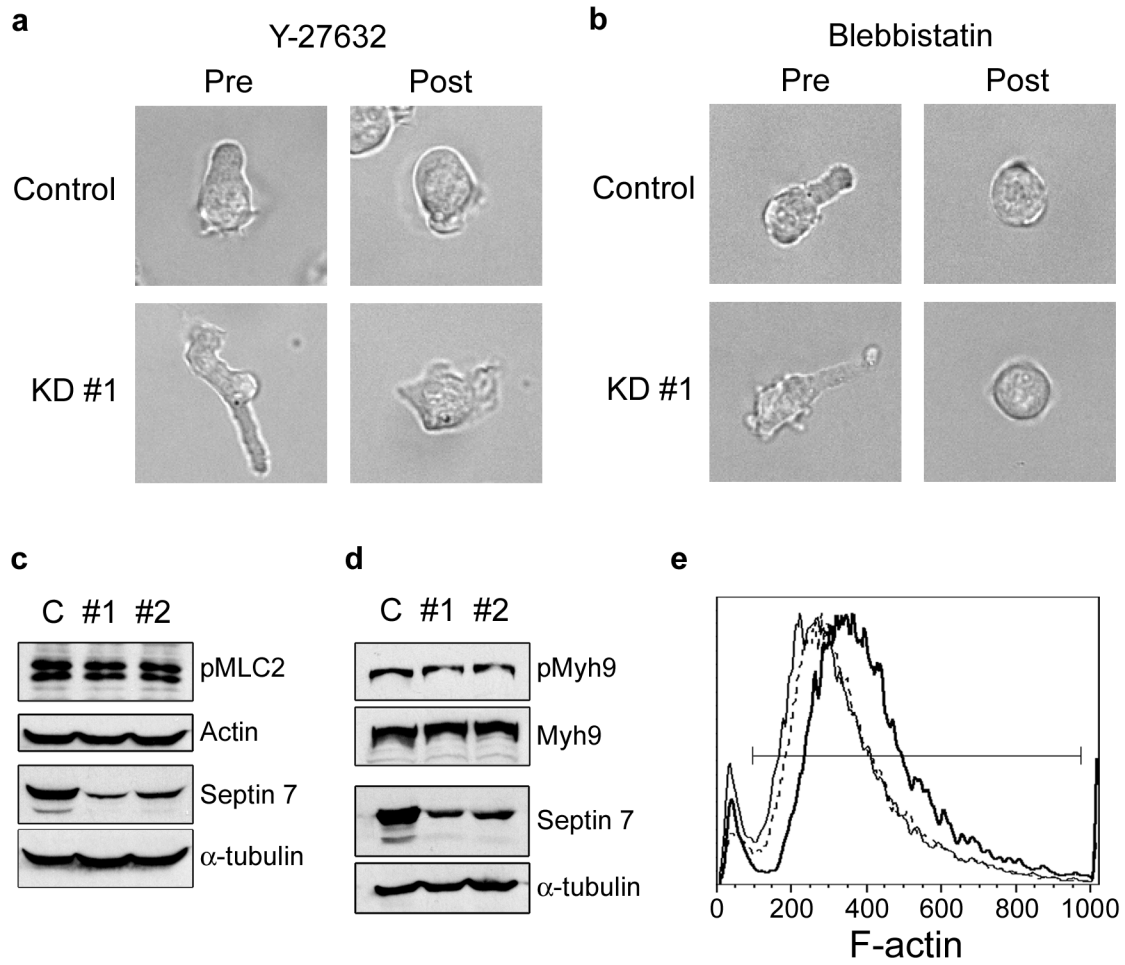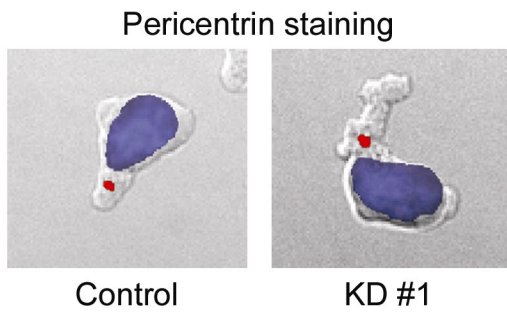
Figure 4 Septins counteract myosin-dependent uropod formation but do not regulate myosin II activity. (**a**, **b**) ROCK and myosin II activity are required for uropod formation in both Sept7 KD and control treated T cells. Treatment of cells with the ROCK inhibitor Y-27632 or with the myosin II inhibitor Blebbistatin resulted in T cell rounding, indicating that these molecules are still required for uropod formation in the absence of septin complexes. T cell rounding was observed in greater than 95% of cells scored for both inhibitors, with at least 84 cells scored from three independent experiments. Results were similar for Sept7 KD #2 (data not shown). (**c**, **d**) Myosin II is not over-active in Sept7 KD T cells. In order to determine if the increased uropod length was due to over-activation of myosin II, we examined phosphorylation of the myosin light chain (pMLC2) and heavy chain (pMyh9). No differences in the basal phosphorylation of MLC2 or Myh9 were observed. (**e**) Sept7 KD T cells have a 10-30% reduction in actin filaments (control = bold line, KD #1 = solid line, KD #2 = dotted line), indicating disruption of the actin cytoskeleton. Levels of total actin were not altered in these cells (shown in **c**). Similar results were obtained in three independent experiments.

a Y-27632

Pre   Post

Control

KD #1

b Blebbistatin

Pre   Post

Control

KD #1

c

C #1 #2

pMLC2

Actin

Septin 7

α-tubulin

d

C #1 #2

pMyh9

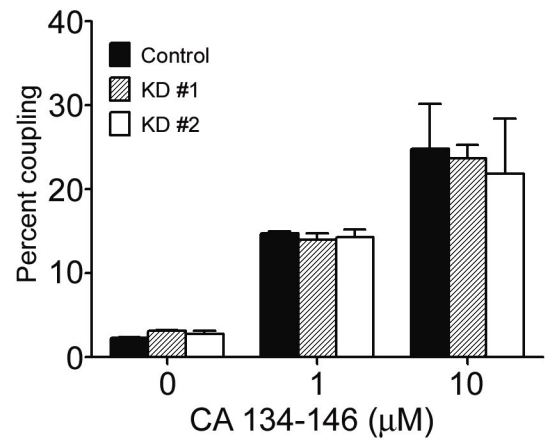Myh9

Septin 7

α-tubulin

e

F-actin

Figure 5 Septins are not required to maintain critical cell polarity but do regulate the ability of T cells to transmigrate through restrictive barriers. (**a**) In order to determine if septins are required to maintain T cell polarity, we examined the location of the MTOC in crawling Sept7 KD T cells using pericentrin as a marker. The MTOC (indicated by red dot) was correctly positioned behind the nucleus (in blue) in greater than 97% of both control and septin deficient cells with at least 34 cells scored. Similar results were obtained for Sept7 KD #2 and when septin deficient T cells were stained for α-tubulin (data not shown). (**b**) Sept7 KD T cells are reactive to antigen-pulsed APCs equivalently to control treated cells, indicating polarity is not affected in the absence of septin complexes. T cells and B cells pulsed with varying concentrations of peptide as indicated were allowed to couple for 45 minutes following a brief initial spin. Couples were then fixed, stained for a B cell specific marker (T cells were GFP positive) and analyzed by flow cytometry. (**c**) Sept7 KD and control T cells are responsive to MIP-1α chemokine gradients in transwell assays. In order for efficient transmigration of D10 T cells, 8 μm pores were used. Although specific chemotaxis is low, Sept7 KD T cells can respond to directional cues similar to control treated T cells. However, Sept7 KD T cells transmigrate through 8 μm pores (± chemokine) approximately two-fold better than control cells. (**d**) Sept7 KD T cells transmigrate through extremely small pores. Since Sept7 KD T cells were able to transmigrate through 8 μm pores more efficiently than control treated T cells, we performed transmigration assays (in the absence of chemokine) using transwells with 3 μm and 5 μm pores. While transmigration was restricted in control treated cells, Sept7 KD T cells transmigrated through both 3 μm and 5 μm pores

approximately five-fold better than control cells. Similar results were obtained in three

independent experiments for (**b, c, d**).

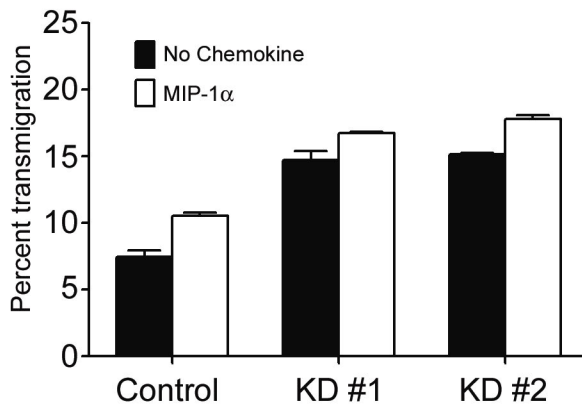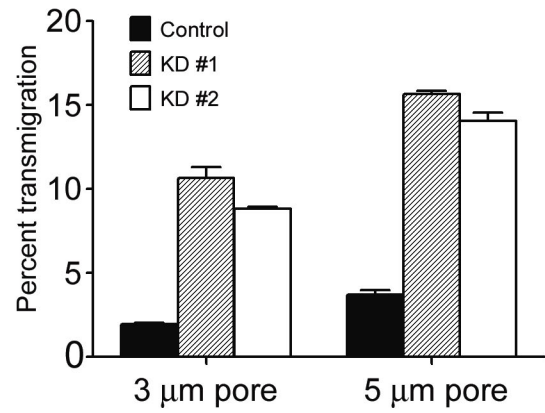**a**

Pericentrin staining

Control   KD #1

b

Percent coupling

- Control
- KD #1
- KD #2

CA 134-146 (µM)

c

Percent transmigration

- No Chemokine
- MIP-1α

Control   KD #1   KD #2

d

Percent transmigration

- Control
- KD #1
- KD #2

3 µm pore   5 µm pore

Supplemental Figure 1 Septin RNA expression in D10 T cells. RNA was isolated from D10 T cells and whole cell extracts from mouse spleen and brain for positive controls. Septin expression was then screened using reverse-transcriptase PCR (RT). Transcripts for all septins tested, except Septins 3 and 5, were present in D10 T cells. Screening primers were designed based on sequence information obtained from the Ensembl database (Supplemental Table 1). Regions common to all known transcripts of individual septins were chosen in order to amplify any possible isoforms expressed in T cells. When multiple transcripts were present, sequences were compared against transcripts found in the GenBank database. Partial mRNA sequence for Septin 12 is present in GenBank (gi:21312733), however, primers designed against that sequence did not amplify a fragment in any of the samples tested. A murine homolog of Septin 13 could not be found via sequence analysis. A putative gene with significant homology to other murine septins was found on chromosome 5 (Ensembl gene ID: ENSMUSG00000034219); however, the expression of this gene was not tested in these samples.
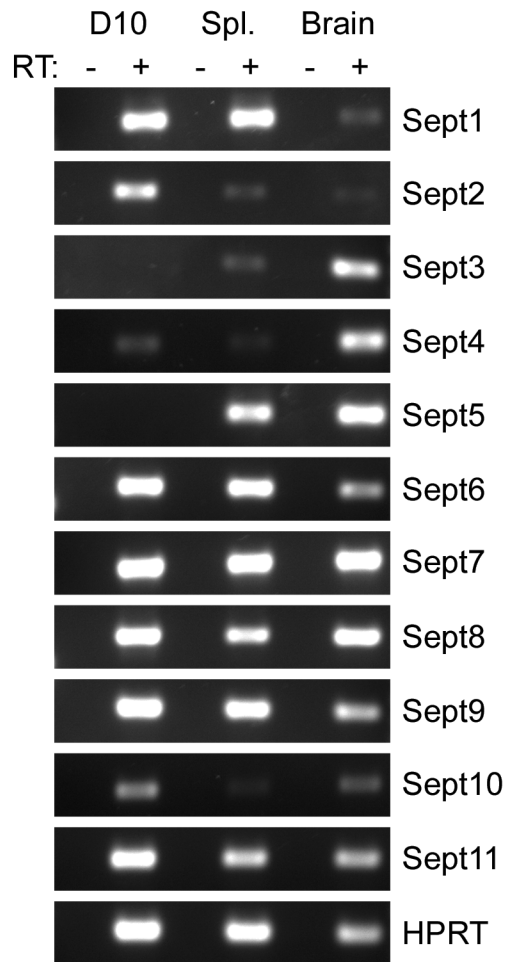
Supplemental Figure 2 Confocal imaging of a septin 'collar' demonstrating punctate nature of septin complexes along the T cell mid-body. Top and side view of a crawling D10 T cell fixed and stained for Sept7. Confocal images were acquired using a 63X objective and three-dimensional reconstructions were compiled using Metamorph software. Distinct punctate dots of Sept7 are found in the T cell mid-body and uropod, indicating the presence of arrayed septin filaments. Bar, 10 μm. A rendered movie of this image is shown as movie SM1.

3D reconstruction

Top view

LE

U

330

60

Side view

Coverslip

64
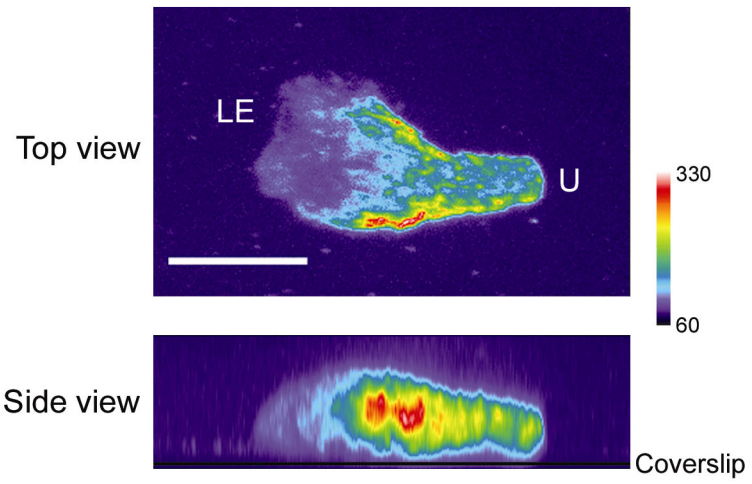
Supplemental Figure 3 Sept7 knock-down (KD) D10 T cells are not defective in cell division. DNA content was examined in Sept7 KD and control treated T cells 72 hours post-transfection in order to determine if Sept7 KD T cells had any defects in cell division. Cells were incubated with 10 µg/ml Hoechst 33342 for 45-90 minutes at 37°C and analyzed on a BD LSR II flow cytometer equipped with a UV laser. Profiles of DNA content of Sept7 KD T cells, KD #1 (solid line) and KD #2 (dashed line, indicated by arrow) were almost identical to control treated cells (bold line), indicating D10 T cells divide normally in the absence of septin complexes.
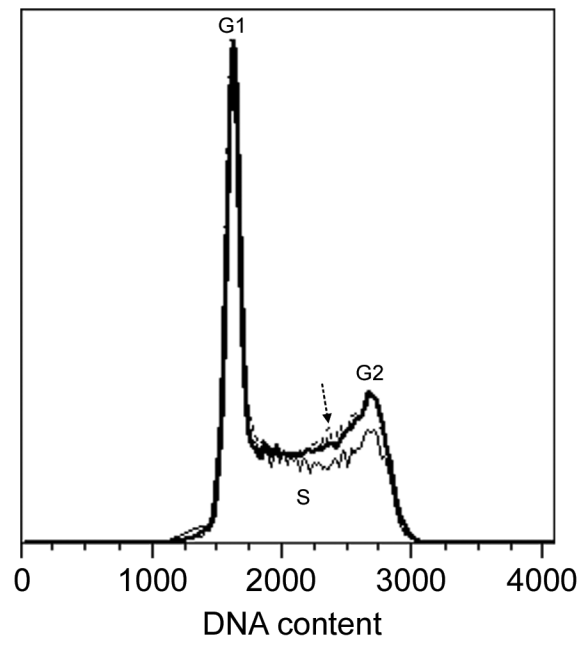
Supplemental Table 1 Primers used for screening septin RNA expression in D10 T cells.

Mouse Septin Gene/Protein	Ensembl Gene ID/ Transcript ID	Chromosome	PCR Primers	Primer Location	Fragment Size (mRNA)
SEPT1/SEPT1	ENSMUSG00000000486	Chr. 7	For: 5' - GTATCAAGGTGAAGTTGACCTTGGTGG - 3'	Exon 3	388 bp
	ENSMUST00000000497		Rev: 5' - TCCTCATCAGAGTCACACTCTGGG - 3'	Exon 8	
SEPT2/SEPT2	ENSMUSG00000026276	Chr. 1	For: 5' - TTCGACTGTTGAGATTGAAGAGCGG - 3'	Exon 5	493 bp
	ENSMUST00000027495		Rev: 5' - TTCAATCAACTGGTTGGAGCCAACC - 3'	Exon 9	
SEPT3/SEPT3	ENSMUSG00000022456	Chr. 15	For: 5' - AAGTCAACACTGGTCAACACCCTC - 3'	Exon 2	397 bp
	ENSMUST00000077804		Rev: 5' - TGACAGGAATGATGTTCACCACTTTGC - 3'	Exon 5	
SEPT4/SEPT4	ENSMUSG00000020486	Chr. 11	For: 5' - AAGGAGTATGTGGGCTTTGCAACC - 3'	Exon 3	292 bp
	ENSMUST00000018544		Rev: 5' - TGTTGTTGACTGCATCCCCAAATCC - 3'	Exon 5	
SEPT5/SEPT5	ENSMUSG00000072214	Chr. 16	For: 5' - TGAAACACACCGTCGACATTGAGG - 3'	Exon 5	398 bp
	ENSMUST00000096987		Rev: 5' - TGGAAACTGGTACACGTGGATCC - 3'	Exon 8	
SEPT6/SEPT6	ENSMUSG00000050379	Chr. X	For: 5' - CAGCTGGTGAATAAGTCAGTCAGCC - 3'	Exon 2	508 bp
	ENSMUST00000060474		Rev: 5' - TGATCTTGAACTTTGCCAGCTCACTC - 3'	Exon 5	
SEPT7/SEPT7	ENSMUSG00000001833	Chr. 9	For: 5' - TCCAGGATTTGGAGATGCAGTGG - 3'	Exon 5	465 bp
	ENSMUST00000060080		Rev: 5' - CAAGGATACTGCCTTCCTCTGACTC - 3'	Exon 9	
SEPT8/SEPT8	ENSMUSG00000018398	Chr. 11	For: 5' - TATCTGCAGGAGGAGTTGAAGATCCG - 3'	Exon 4	615 bp
	ENSMUST00000018542		Rev: 5' - GCTTAGGAACTCCTTCCTCTTTGCC - 3'	Exon 8	
SEPT9/SEPT9	ENSMUSG00000059248	Chr. 11	For: 5' - AGACGATCGAAATCAAGTCGATCACC - 3'	Exon 4	430 bp
	ENSMUST00000019038		Rev: 5' - TCCTCATCAAACTCCTTCTGCGG - 3'	Exon 8	
SEPT10/SEPT10	ENSMUSG00000019917	Chr. 10	For: 5' - AGGAAGAACTGAAGATCAAGCGTGC - 3'	Exon 3	493 bp
	ENSMUST00000089092		Rev: 5' - TAGTGCCTCATATGTGTCTGCTCCC - 3'	Exon 6	
SEPT11/SEPT11	ENSMUSG00000058013	Chr. 5	For: 5' - ATGACACAAGGATTCACGCCTGC - 3'	Exon 4	464 bp
	ENSMUST00000074733		Rev: 5' - ATACAACTCGTAGTGGCGAGTGTGC - 3'	Exon 7	

Figure legends for supplemental movies

Supplemental Movie SM1 A three-dimensional rendering of annular and cortical septin bundles. The cell from Figure S2 was rendered using a maximal intensity projection algorithm to generate a three-dimensional reconstruction.

Supplemental Movie SM2 Crawling of control treated D10 T cells. In order to examine membrane dynamics in control treated T cells, time-lapse images were acquired at 5-10 second intervals for at least 10 minutes. Imaging was performed in 0.25% low-melting point agarose to limit drifting of non-adherent cells.

Supplemental Movie SM3 Membrane blebbing in Sept7 KD D10 T cells. In order to examine membrane dynamics in septin deficient T cells, time-lapse images were acquired at 5-10 second intervals for at least 10 minutes. Membrane blebbing is indicated by arrows during the movie. Imaging was performed in 0.25% low-melting point agarose to limit drifting of non-adherent cells.

Supplemental Movie SM4 Excess protrusions in Sept7 KD D10 T cells. In order to examine membrane dynamics in septin deficient T cells, time-lapse images were acquired at 5-10 second intervals for at least 10 minutes. Excess protrusions are observed for two different cells during the movie and are indicated by arrows. Imaging was performed in 0.25% low-melting point agarose to limit drifting of non-adherent cells.

Supplemental Movie SM5 ROCK activity is still required for uropod formation in control and Sept7 KD D10 T cells. In order to determine if ROCK activity was still required for uropod formation in septin deficient T cells, control and Sept7 KD T cells were treated with the ROCK inhibitor Y-27632. Time-lapse images were acquired at 30-second intervals with addition of the drug after time-point five. Imaging was performed in 0.10% low-melting point agarose to limit drifting of non-adherent cells.

Supplemental Movie SM6 Myosin II activity is still required for uropod formation in control and Sept7 KD D10 T cells. In order to determine if myosin II activity was still required for uropod formation in septin deficient T cells, control and Sept7 KD T cells were treated with the myosin II inhibitor Blebbistatin. Time-lapse images were acquired at 30-second intervals immediately after addition of the drug. Imaging was performed in 0.10% low-melting point agarose to limit drifting of non-adherent cells.

Chapter 4:

Concluding Remarks

Discussion

This is the first study to examine the function of septin complexes in T cell crawling and morphology. In D10 T cells, septin complexes are enriched in the T cell mid-body and act as a structural scaffold to limit both anterior and posterior protrusions. In the absence of septin complexes, the length of the uropod is increased and the plasma membrane exhibits structural instabilities, resulting in membrane blebbing and the presence of excess protrusions. Finally, septin deficient D10 T cells have the ability to transmigrate through extremely small pores, indicating that septins provide a structural scaffold to maintain rigidity in wild-type T cells.

T cells deficient in septin complexes have a dramatic increase in uropod length; however, the underlying molecular mechanisms for this increase are not clear. In addition, there was also a considerable amount of variation in the length of the uropod in Sept7 knock-down (KD) D10 T cells, with some cells having a two and a half to three fold increase in uropod length (Chapter 3, Figure 3). In this study, the level of GFP expression could not be used to correlate the level of knock-down in individual cells, as the GFP marker was not expressed from the same plasmid as the shRNA. A plasmid that expresses both the GFP marker and the shRNA could be used to determine if the increase in uropod length correlates with the level of knock-down in individual D10 T cells. If this is indeed the case, this would further support the hypothesis that septins are required to confine and restrict the length of the uropod.

All of these studies were performed *in vitro* using the T cell clone, D10.G4. For studying

T cell biology, this clone has several advantages and disadvantages that limit the types of

experiments that can be performed. First, D10 T cells exhibit a highly polarized

phenotype and actively migrate, making them an ideal cell line to study T cell crawling

and morphology. Second, they are easy to grow and transfect well, a good combination

when large quantities of cells are needed for experiments. This was extremely

advantageous for generating D10 T cells deficient in septin complexes.

However, D10 T cells also have several disadvantages that limit the questions that can be

answered. For example, D10 T cells do not actively crawl when transferred into mice

(data not shown); therefore, the effects of septin KD could not be examined *in vivo*. As

shown in Chapter 3 Figure 6, D10 T cells do not respond well to chemokines (specific

chemotaxis is low), making it difficult to determine if defects in chemotaxis are indeed

present in Sept7 KD D10 T cells due to the poor dynamic range. In addition, D10 T cells

do not transmigrate through transwells coated with endothelial cells (data not shown), so

the role of septins in transendothelial migration could not be tested *in vitro*. Finally, the

subclone of D10 T cells used for this study does not require antigen stimulation for

growth; therefore, the role of septins in T cell activation and proliferation could not be

tested either.

Repeating these experiments in T cell blasts using a retroviral delivery system (or

nucleofection from Amaxa Biosystems) to generate septin deficient T cells would allow

many of these questions to be addressed. Although Sept7 KD D10 T cells do not show

dramatic defects in crawling *in vitro*, these defects might be enhanced *in vivo* where cells

are forced to crawl in a three-dimensional environment packed full of other cells. Recent

advances in two-photon microscopy allow T cell crawling to be examined *in vivo* in

intake lymph nodes (Miller et al., 2002). These experiments would also allow the role of

septins in transendothelial migration to be examined *in vivo*. It would be interesting to see

if Sept7 KD T cells are capable of entering lymph nodes similar to control treated cells.

Considering Sept7 KD D10 T cells can transmigrate through smaller pores *in vitro*, one

could hypothesize a similar result *in vivo*. However, if septin complexes are truly

required for structural support, septin deficient T cells may have problems withstanding

sheer flow *in vivo* and may not be able to exit the bloodstream.

Potential roles of septins in T cell activation

T cell activation involves the interaction of the T cell receptor (TCR) with cognate

peptide-MHC complexes on antigen presenting cells (APCs). TCR recognition results in

downstream signaling cascades important for T cell activation, proliferation and gain of

effector functions. At the junction between the T cell and the APC, a highly ordered

structure of signaling and adhesion molecules forms what is known as the immunological

synapse (IS) (Krummel et a., 2000; Monks et al., 1998). The IS is characterized by the

accumulation of the TCR and its associated signaling complex CD3 at the center of the

contact (also known as the central supramolecular activation cluster or c-SMAC)

surrounded by a ring of adhesion molecules including LFA-1 (also know as peripheral

supramoleculer activation cluster or p-SMAC). While many of the molecules involved in

IS formation and TCR signaling are known, the exact function of the IS is still controversial.

When a T cell encounters an APC bearing its cognate peptide-MHC complex, dramatic changes in T cell morphology ensue. TCR signaling induces T cell stopping and morphological changes that result in the loss of the uropod and T cell rounding (one potential mechanism is discussed in Jacobelli et al., 2004). These events most likely occur through inactivation of myosin II and de-phosphorylation of ERM proteins (reviewed in Krummel and Macara, 2006). In addition, there is a global re-organization of actin filaments, microtubules and cytoplasmic and membrane proteins. This includes re-orientation of the MTOC in front of the nucleus, such that it is positioned directly behind the IS. Interestingly, septins accumulate and form a ring at the p-SMAC during IS formation (Figure 1a, b and c). The role of septins in T cell activation and in formation or maintenance of the IS has not been determined. The presence of a septin ring confining the IS has several implications worth further investigation.

In budding yeast, septins function as both scaffolds to attract proteins to the mother-bud neck and as diffusion barriers to confine molecules to this region during cell division (Dobbelaere and Barral, 2004; reviewed in Versele and Thorner, 2005). Although it has not been directly shown, a similar function has been postulated for mammalian septins during cell division (Schmidt and Nichols, 2004), and septins have been shown to act as a diffusion barrier in the mammalian sperm tail (Ihara et al., 2005; Kissel et al., 2005).

Whether septins serve a similar function to restrict molecules from entering or exiting the IS has not been examined.

Following cytokinesis, septins are also required for abscission in budding yeast (Dobbelaere and Barral, 2004), a process that requires the exocyst complex and the delivery and fusion of vesicles for membrane resolution. It has been hypothesized that septins are required to recruit or confine the exocyst complex to the mother-bud neck. A similar result has been observed in mammalian cells (Surka et al., 2002), indicating that septins may play an evolutionarily conserved role in this process. In mammalian cells, septins also bind the exocyst complex (Sec6/8) and SNARE proteins (t-SNARES), both of which are required for vesicle trafficking and fusion (reviewed in Joo et al., 2005). Interestingly, polarized exocytosis at the IS has been observed for cytokines (such as interleukin-2 and interferon-γ) and for cytotoxic granules important for CD8+ T cell killing (reviewed in Krummel and Macara, 2006). Therefore, it is possible that septins play a role in the localization or confinement of vesicles to the IS.

Conclusion

This study examined the role of septin complexes in T cell morphology and crawling. Septin complexes are important components of the T cell cytoskeleton and are required for structural stability and normal polarized T cell morphology. T cells deficient in septin complexes have a dramatic increase in uropod length and exhibit defects in membrane integrity. In addition, septin deficient T cells can transmigrate through extremely small pores, a result that has implications for transendothelial migration and potentially tumor

metastasis. Future studies will hopefully provide additional insights into how septin

complexes function in T cell crawling and activation, both *in vitro* and *in vivo*.

Figure 1 Septins polarize to the immunological synapse during T cell activation. (**a**, **b** and **c**) D011.10 T cells and A20 B cells pulsed with D011.10 specific peptides were incubated together on slides for 30 min before being fixed and stained with anti-CD3 (clone 500A2) and anti-Sept1 or anti-Sept7 antibodies. T cell-APC conjugates were scored for the presence of either a central accumulation of CD3 (c-smac) or the presence of a peripheral septin ring around the contact face (p-smac). (**a**) Examples of T cell-APC conjugates with a central CD3 c-smac surrounded by a peripheral ring of septin. Right, 3D reconstructions of the interface between the T cells and the APCs (contact face), demonstrating a distinct CD3 c-smac surround by a peripheral septin ring. (**b**) Peripheral septin rings form in the absence of a clear CD3 c-smac. Conjugates were found that contained a defined peripheral septin ring with only partial or no apparent polarization of CD3. (**c**) Scoring of T cell-APC conjugates demonstrating the majority of interactions involve clear polarization of both CD3 and septins. However, septin rings were present in the absence of a centralized CD3 c-smac, indicating septin rings form before c-smac formation.

a

DIC	CD3	Septin 1	Merge	Interface

b

	DIC	CD3	Septin 7	Merge
Partial CD3 polarization				
CD3 non-polarized				

c

Percent observed

☐ Sept1
■ Sept7

| Septin p-smac: | + | + | - |
| CD3 c-smac: | + | - | + |
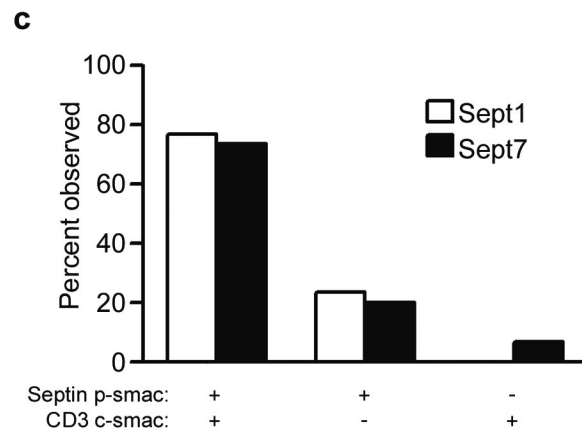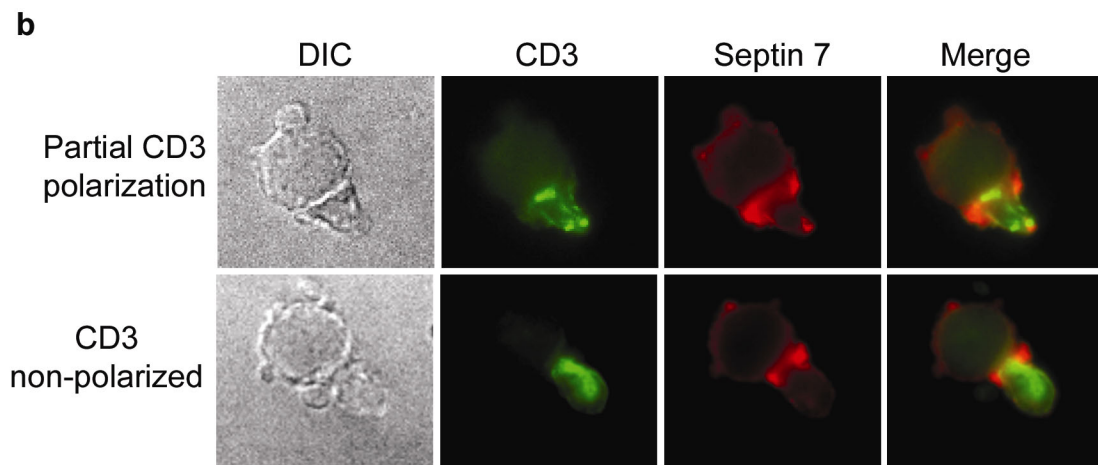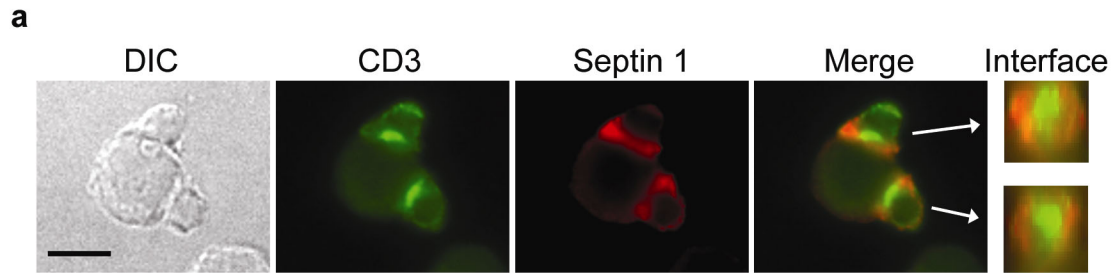
References

Bajenoff M, Egen JG, Koo LY, Laugier JP, Brau F, Glaichenhaus N, Germain RN. (2006) Stromal cell networks regulate lymphocyte entry, migration, and territoriality in lymph nodes. *Immunity*. 25(6):989-1001.

Cau J, Hall A. (2005) Cdc42 controls the polarity of the actin and microtubule cytoskeletons through two distinct signal transduction pathways. *J Cell Sci*. 118(Pt 12):2579-87.

Chacko AD, Hyland PL, McDade SS, Hamilton PW, Russell SH, Hall PA. (2005) SEPT9_v4 expression induces morphological change, increased motility and disturbed polarity. *J Pathol*. 206(4):458-65.

Dobbelaere J, Barral Y. (2004) Spatial coordination of cytokinetic events by compartmentalization of the cell cortex. *Science*. 305(5682):393-6.

Dulyaninova NG, Malashkevich VN, Almo SC, Bresnick AR. (2005) Regulation of myosin-IIA assembly and Mts1 binding by heavy chain phosphorylation. *Biochemistry*. 44(18):6867-76.

Ebert LM, Schaerli P, Moser B. (2005) Chemokine-mediated control of T cell traffic in lymphoid and peripheral tissues. *Mol Immunol*. 42(7):799-809

Field CM, Coughlin M, Doberstein S, Marty T, Sullivan W. (2005) Characterization of anillin mutants reveals essential roles in septin localization and plasma membrane integrity. *Development*. 132(12):2849-60.

Friedl P. (2004) Prespecification and plasticity: shifting mechanisms of cell migration. *Curr Opin Cell Biol*. 16(1):14-23.

Gladfelter AS, Kozubowski L, Zyla TR, Lew DJ. (2005) Interplay between septin organization, cell cycle and cell shape in yeast. *J Cell Sci*. 118(Pt 8):1617-28.

Gomes ER, Jani S, Gundersen GG. (2005) Nuclear movement regulated by Cdc42, MRCK, myosin, and actin flow establishes MTOC polarization in migrating cells. *Cell*. 121(3):451-63.

Hall PA, Jung K, Hillan KJ, Russell SE. (2005) Expression profiling the human septin gene family. *J Pathol*. 206(3):269-78.

Hall PA, Russell SE. (2004) The pathobiology of the septin gene family. *J Pathol*. 204(4):489-505.

Hordijk PL. (2006) Endothelial signalling events during leukocyte transmigration. *FEBS J*. 273(19):4408-15.

Ihara M, Kinoshita A, Yamada S, Tanaka H, Tanigaki A, Kitano A, Goto M, Okubo K, Nishiyama H, Ogawa O, Takahashi C, Itohara S, Nishimune Y, Noda M, Kinoshita M. (2005) Cortical organization by the septin cytoskeleton is essential for structural and mechanical integrity of mammalian spermatozoa. *Dev Cell*. 8(3):343-52.

Ito H, Iwamoto I, Morishita R, Nozawa Y, Narumiya S, Asano T, Nagata K. (2005) Possible role of Rho/Rhotekin signaling in mammalian septin organization. *Oncogene*. 24(47):7064-72.

Jacobelli J, Chmura SA, Buxton DB, Davis MM, Krummel MF. (2004) A single class II myosin modulates T cell motility and stopping, but not synapse formation. *Nat Immunol*. 5(5):531-8.

Joberty G, Perlungher RR, Sheffield PJ, Kinoshita M, Noda M, Haystead T, Macara IG. (2001) Borg proteins control septin organization and are negatively regulated by Cdc42. *Nat Cell Biol*. 3(10):861-6.

Joo E, Tsang CW, Trimble WS. (2005) Septins: traffic control at the cytokinesis intersection. *Traffic*. 6(8):626-34.

Kinoshita M. (2006) Diversity of septin scaffolds. *Curr Opin Cell Biol*. 18(1):54-60.

Kinoshita M, Field CM, Coughlin ML, Straight AF, Mitchison TJ. (2002) Self- and actin templated assembly of Mammalian septins. *Dev Cell*. 3(6):791-802.

Kissel H, Georgescu MM, Larisch S, Manova K, Hunnicutt GR, Steller H. (2005) The Sept4 septin locus is required for sperm terminal differentiation in mice. *Dev Cell*. 8(3):353-64.

Koshland D, Kent JC, Hartwell LH. (1985) Genetic analysis of the mitotic transmission of minichromosomes. *Cell*. 40(2):393-403.

Kremer BE, Haystead T, Macara IG. (2005) Mammalian septins regulate microtubule stability through interaction with the microtubule-binding protein MAP4. *Mol Biol Cell*. 16(10):4648-59.

Krummel MF, Macara I. (2006) Maintenance and modulation of T cell polarity. *Nat Immunol*. 7(11):1143-9.

Krummel MF, Sjaastad MD, Wulfing C, Davis MM. (2000) Differential clustering of CD4 and CD3zeta during T cell recognition. *Science*. 289(5483):1349-52.

Lee JH, Katakai T, Hara T, Gonda H, Sugai M, Shimizu A. (2004) Roles of p-ERM and Rho-ROCK signaling in lymphocyte polarity and uropod formation. *J Cell Biol*. 167(2):327-37.

Leitges M, Sanz L, Martin P, Duran A, Braun U, Garcia JF, Camacho F, Diaz-Meco MT, Rennert PD, Moscat J. (2001) Targeted disruption of the zetaPKC gene results in the impairment of the NF-kappaB pathway. *Mol Cell*. 8(4):771-80.

Longtine MS, Fares H, Pringle JR. (1998) Role of the yeast Gin4p protein kinase in septin assembly and the relationship between septin assembly and septin function. *J Cell Biol*. 143(3):719-36.

Ludford-Menting MJ, Oliaro J, Sacirbegovic F, Cheah ET, Pedersen N, Thomas SJ, Pasam A, Iazzolino R, Dow LE, Waterhouse NJ, Murphy A, Ellis S, Smyth MJ, Kershaw MH, Darcy PK, Humbert PO, Russell SM. (2005) A network of PDZ-containing proteins regulates T cell polarity and morphology during migration and immunological synapse formation. *Immunity*. 22(6):737-48.

Macara IG, Baldarelli R, Field CM, Glotzer M, Hayashi Y, Hsu SC, Kennedy MB, Kinoshita M, Longtine M, Low C, Maltais LJ, McKenzie L, Mitchison TJ, Nishikawa T, Noda M, Petty EM, Peifer M, Pringle JR, Robinson PJ, Roth D, Russell SE, Stuhlmann H, Tanaka M, Tanaka T, Trimble WS, Ware J, Zeleznik-Le NJ, Zieger B. (2002) Mammalian septins nomenclature. *Mol Biol Cell*. 13(12):4111-3.

Miller MJ, Wei SH, Parker I, Cahalan MD. (2002) Two-photon imaging of lymphocyte motility and antigen response in intact lymph node. *Science*. 296(5574):1869-73.

Monks CR, Freiberg BA, Kupfer H, Sciaky N, Kupfer A. (1998) Three-dimensional segregation of supramolecular activation clusters in T cells. *Nature*. 395(6697):82-6.

Nagata K, Asano T, Nozawa Y, Inagaki M. (2004) Biochemical and cell biological analyses of a mammalian septin complex, Sept7/9b/11. *J Biol Chem*. 279(53):55895-904.

Nagata K, Inagaki M. (2005) Cytoskeletal modification of Rho guanine nucleotide exchange factor activity: identification of a Rho guanine nucleotide exchange factor as a binding partner for Sept9b, a mammalian septin. *Oncogene*. 24(1):65-76.

Nagata K, Kawajiri A, Matsui S, Takagishi M, Shiromizu T, Saitoh N, Izawa I, Kiyono T, Itoh TJ, Hotani H, Inagaki M. (2003) Filament formation of MSF-A, a mammalian septin, in human mammary epithelial cells depends on interactions with microtubules. *J Biol Chem*. 278(20):18538-43.

Nourshargh S, Marelli-Berg FM. (2005) Transmigration through venular walls: a key regulator of leukocyte phenotype and function. *Trends Immunol*. 26(3):157-65.

Osaka M, Rowley JD, Zeleznik-Le NJ. (1999) MSF (MLL septin-like fusion), a fusion partner gene of MLL, in a therapy-related acute myeloid leukemia with a t(11;17)(q23;q25). *Proc Natl Acad Sci U S A*. 96(11):6428-33.

81

Raftopoulou M, Hall A. (2004) Cell migration: Rho GTPases lead the way. *Dev Biol*. 265(1):23-32.

Ratner S, Piechocki MP, Galy A. (2003) Role of Rho-family GTPase Cdc42 in polarized expression of lymphocyte appendages. *J Leukoc Biol*. 73(6):830-40.

Robertson C, Church SW, Nagar HA, Price J, Hall PA, Russell SE. (2004) Properties of SEPT9 isoforms and the requirement for GTP binding. *J Pathol*. 203(1):519-27.

Rodal AA, Kozubowski L, Goode BL, Drubin DG, Hartwig JH. (2005) Actin and septin ultrastructures at the budding yeast cell cortex. *Mol Biol Cell*. 16(1):372-84.

Round JL, Tomassian T, Zhang M, Patel V, Schoenberger SP, Miceli MC. (2005) Dlgh1 coordinates actin polymerization, synaptic T cell receptor and lipid raft aggregation, and effector function in T cells. *J Exp Med*. 201(3):419-30.

Russell SE, Hall PA. (2005) Do septins have a role in cancer? *Br J Cancer*. 93(5):499-503.

Russell SE, McIlhatton MA, Burrows JF, Donaghy PG, Chanduloy S, Petty EM, Kalikin LM, Church SW, McIlroy S, Harkin DP, Keilty GW, Cranston AN, Weissenbach J, Hickey I, Johnston PG. (2000) Isolation and mapping of a human septin gene to a region on chromosome 17q, commonly deleted in sporadic epithelial ovarian tumors. *Cancer Res*. 60(17):4729-34.

Samstag Y, Eibert SM, Klemke M, Wabnitz GH. (2003) Actin cytoskeletal dynamics in T lymphocyte activation and migration. *J Leukoc Biol*. 73(1):30-48.

Sanchez-Madrid F, del Pozo MA. (1999) Leukocyte polarization in cell migration and immune interactions. *EMBO J*. 18(3):501-11.

Schmidt K, Nichols BJ. (2004) A barrier to lateral diffusion in the cleavage furrow of dividing mammalian cells. *Curr Biol*. 14(11):1002-6.

Schwartz M. (2004) Rho signalling at a glance. *J Cell Sci*. 117(Pt 23):5457-8.

Scott M, Hyland PL, McGregor G, Hillan KJ, Russell SE, Hall PA. (2005) Multimodality expression profiling shows SEPT9 to be overexpressed in a wide range of human tumours. *Oncogene*. 24(29):4688-700.

Sheffield PJ, Oliver CJ, Kremer BE, Sheng S, Shao Z, Macara IG. (2003) Borg/septin interactions and the assembly of mammalian septin heterodimers, trimers, and filaments. *J Biol Chem*. 278(5):3483-8.

Sorensen AB, Lund AH, Ethelberg S, Copeland NG, Jenkins NA, Pedersen FS. (2000) Sint1, a common integration site in SL3-3-induced T-cell lymphomas, harbors a putative proto-oncogene with homology to the septin gene family. *J Virol.* 74(5):2161-8.

Spiliotis ET, Kinoshita M, Nelson WJ. (2005) A mitotic septin scaffold required for Mammalian chromosome congression and segregation. *Science*. 307(5716):1781-5.

Spiliotis ET, Nelson WJ. (2006) Here come the septins: novel polymers that coordinate intracellular functions and organization. *J Cell Sci.* 119(Pt 1):4-10.

Straight AF, Cheung A, Limouze J, Chen I, Westwood NJ, Sellers JR, Mitchison TJ. (2003) Dissecting temporal and spatial control of cytokinesis with a myosin II Inhibitor. *Science*. 299(5613):1743-7.

Surka MC, Tsang CW, Trimble WS. (2002) The mammalian septin MSF localizes with microtubules and is required for completion of cytokinesis. *Mol Biol Cell*. 13(10):3532-45.

Takizawa PA, DeRisi JL, Wilhelm JE, Vale RD. (2000) Plasma membrane compartmentalization in yeast by messenger RNA transport and a septin diffusion barrier. *Science*. 290(5490):341-4.

Tooley AJ, Jacobelli J, Moldovan MC, Douglas A, Krummel MF. (2005) T cell synapse assembly: proteins, motors and the underlying cell biology. *Semin Immunol*. 17(1):65-75.
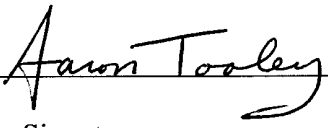
Versele M, Thorner J. (2005) Some assembly required: yeast septins provide the instruction manual. *Trends Cell Biol*. 15(8):414-24.

Publishing Agreement

It is the policy of the University to encourage the distribution of all theses and dissertations. Copies of all UCSF theses and dissertations will be routed to the library via the Graduate Division. The library will make all theses and dissertations accessible· to the public and will preserve these to the best of their abilities, in perpetuity.

Please sign the following statement:

I hereby grant permission to the Graduate Division of the University of California, San Francisco to release copies of my thesis or dissertation to the Campus Library to provide access and preservation, in whole or in part, in perpetuity.

___Aaron Tooley___   ___5/7/2007___

Author Signature   Date